Clays and Clay Minerals, Vol. 58, No. 1, 120–141, 2010.

MINERALOGY, GEOCHEMISTRY, AND ORIGIN OF BENTONITE IN UPPER CRETACEOUS PYROCLASTIC UNITS OF THE TİREBOLU AREA, GİRESUN, NORTHEAST TURKEY

MEHMET ARSLAN[1,*], EMEL ABDİOĞLU[1], AND SELAHATTİN KADİR[2]

[1] Department of Geological Engineering, Karadeniz Technical University, TR-61080 Trabzon, Turkey
[2] Department of Geological Engineering, Eskişehir Osmangazi University, TR-26480 Eskişehir, Turkey

Abstract—Widespread alteration in the Upper Cretaceous pyroclastic units of the Tirebolu (Giresun) area, NE Turkey, has resulted in significant occurrences of bentonite with economic potential. No detailed geological, mineralogical, or geochemical characterization of these occurrences has been carried out to date. The aim of this study was to describe the geological background, the mineralogical, chemical, and stable-isotope characteristics of the bentonite, and major aspects of their formation, *e.g.* type and source of low-temperature alteration, mass balance, chemical evolution of the smectites, and geochemistry of major and trace elements. The bentonite contains abundant smectite with occasional kaolinite and mordenite, volcanogenic feldspar, quartz, biotite, hornblende, glass shards, and pumice fragments, along with the diagenetic minerals, opal-CT, and, in some locations, calcite. X-ray diffraction patterns of the clay fractions exhibit characteristics of pure montmorillonite and beidellite-type smectite. Micromorphologically, the smectite exhibits a honeycomb texture, the kaolinite occurs in both vermiform and irregular platy forms, and the mordenite occurs in fibrous form. All of these minerals are edged with devitrified volcanic glass and resorbed feldspar. Chemically, the smectites are Ca-smectite. Geochemical data indicate that alteration of the pyroclastic units took place under suboxic and anoxic environmental conditions during bentonite formation. Field observations and mineralogical, geochemical, oxygen, and hydrogen isotopic data indicate that the alteration of feldspar and volcanic glass in the pyroclastics by mixed meteoric and sea water in a shallow marine environment under alkaline and acidic conditions, respectively, controlled by environmental Al, Ca, and Na concentrations, resulted in the formation of authigenic smectite, mordenite, and kaolinite. A large Ca content in the smectite originated from surrounding units, which resulted in high alkalinity; Mg originated from seawater.

Key Words—Bentonite, Diagenetic Alteration, Eastern Black Sea, Geochemistry, Mineralogy, Pyroclastics, Smectite, Stable Isotopes, Tirebolu, Turkey.

INTRODUCTION

Widespread bentonite deposits throughout the world occur either by hydrothermal or diagenetic alteration of pyroclastics of intermediate to acidic character (*e.g.* Christidis *et al.*, 1995; Christidis and Dunham, 1997; Christidis and Scott, 1997; Christidis, 1998; Yalçın and Gümüşer, 2000; Ddani *et al.*, 2005; Caballero *et al.*, 2005; Abdioğlu and Arslan, 2005; Christidis and Huff, 2009).

Bentonite is used in many important industrial applications including pelletizing of iron-ore, foundry mouldings, and oil-well drilling fluids (Harvey and Lagaly, 2006; Murray, 2007). White bentonites, which are rarer, have greater market value than other types. The main producing areas of white bentonites are in the USA and in Mediterranean countries such as Greece, Italy, Spain, and Turkey (Christidis and Scott, 1997; Caballero *et al.*, 2005). Despite the increasing industrial and geological importance of these bentonites (*e.g.* Grim and Güven, 1978; Murray, 1991, 1999, 2007; Güven, 2009), only limited detailed studies have been published about the geological features and significance of the clay occurrences in the Eastern Black Sea region, northeastern Turkey (Yalçın and Gümüşer, 2000; Abdioğlu, 2002; Uz *et al.*, 2003; Abdioğlu and Arslan, 2005; Arslan *et al.*, 2006).

Although the alteration in the Eastern Black Sea region (NE Turkey) is related to a massive sulfide deposit in the Upper Cretaceous volcanic units, the lack of hydrothermal features such as mineralogical and geochemical zonation, Fe oxides and/or hydroxides and sulfur phases controlled by faults (Inoue, 1995; Meunier, 1995; 2005; Kadir and Akbulut, 2009; Kadir and Kart, 2009) in the Tirebolu area suggests that the origin of the bentonite in this area is still open to debate. The alteration profiles in the Tirebolu area (NE Turkey) where Upper Cretaceous intermediate to acidic pyroclastics converted to bentonite in a marine environment were examined in the present study, which also combined mineralogical and geochemical analyses in order to investigate the composition and oxygen-hydrogen isotopic characteristics of the bentonites in the area.

* E-mail address of corresponding author:
marslan@ktu.edu.tr
DOI: 10.1346/CCMN.2010.0580112

This study aimed to: (1) define the mineralogy of the bentonites in detail, especially changes in clay mineralogy and associated non-clay minerals; (2) characterize the distribution of major and trace elements in the smectite-rich bentonites and surrounding rocks; and (3) assess the source of the bentonites and their formation conditions.

METHODS

In order to identify the distribution of bentonite in the Tirebolu area, 105 samples of fresh and altered rocks of the Tirebolu formation were collected (Figure 1). The samples were analyzed for their mineralogical characteristics by polarized-light microscopy (Leitz Laborlux 11 Pol), X-ray powder diffractometry (XRD) (Rigaku-DMAXIIC and Rigaku-Geigerflex models), scanning electron microscopy (SEM-EDX, JEOL JSM 84A-EDX), and differential thermal analysis-thermal gravimetry (DTA-TG, Rigaku TAS 100 E and NETZSCH 404 models). The XRD analyses were performed using CuKα radiation and a scanning speed of 1º2θ/min. Random samples of powdered whole-rock samples were used to determine bulk mineralogy. A clay concentrate was obtained by dispersion of the bulk samples in water followed by sedimentation to obtain the 2 μm fraction which was then redispersed overnight in distilled water and separated by centrifugation. The precipitated particles were redispersed in deionized water using ultrasonic vibration for ~15 min. Oriented specimens of the <2 μm fraction were then prepared from each sample. Each of the oriented samples prepared in this fashion was

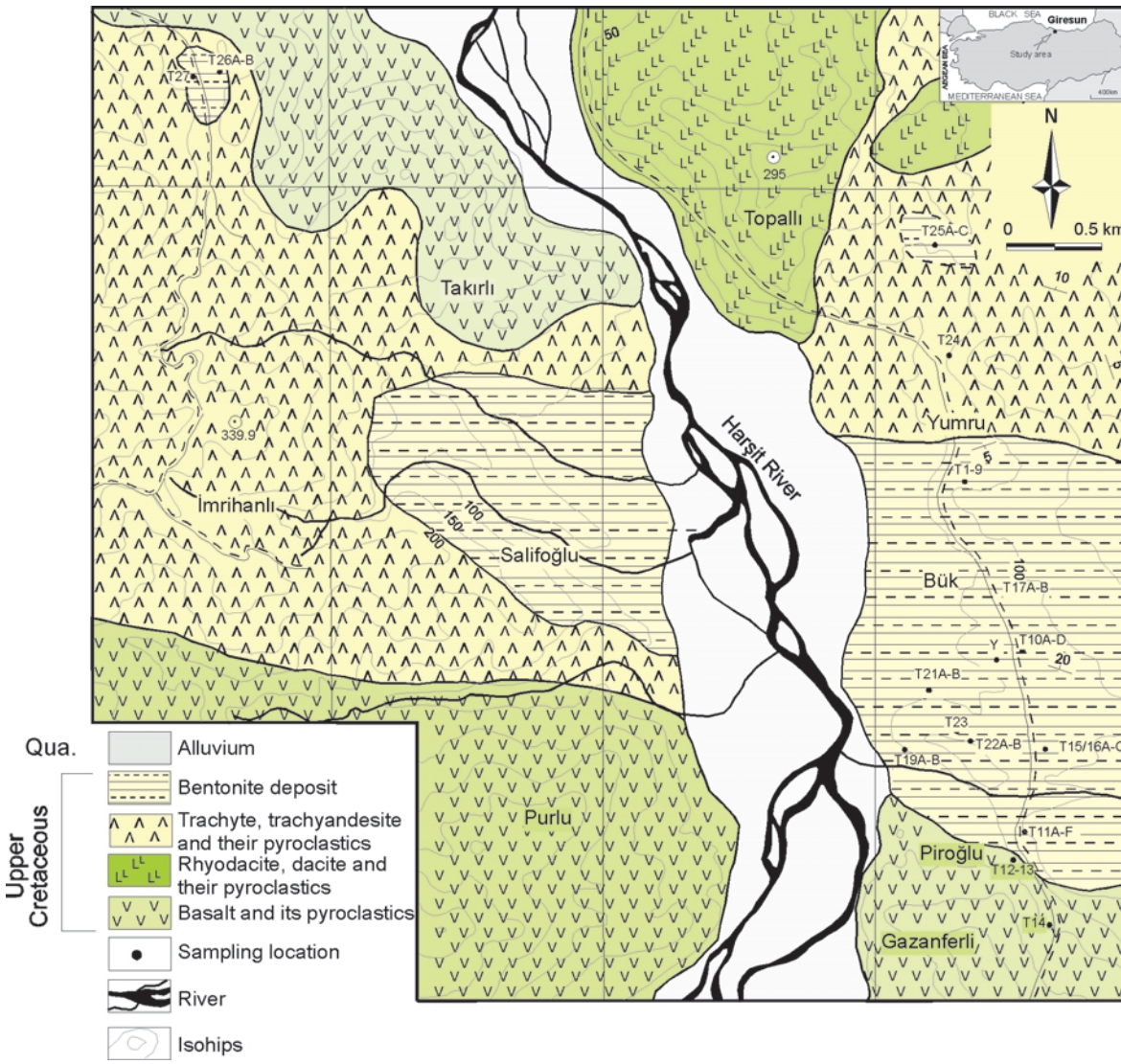

Figure 1. Location and simplified geological map of the study area in the vicinity of Harşit valley, Tirebolu (Giresun), NE Turkey.

https://doi.org/10.1346/CCMN.2010.0580112 Published online by Cambridge University Press

subjected to one of the following treatments: drying only or air drying followed by ethylene glycol solvation at 60ºC for 2 h, and thermal treatment at 350ºC and 550ºC for 2 h. In addition, samples of the 2 μm fraction were also Mg-saturated, Mg-saturated + ethylene glycol solvated, K-saturated, K-saturated + thermally treated at 350ºC or 490ºC, or Li-saturated. Semi-quantitative relative abundances of rock-forming minerals were obtained according to Brindley (1980), and the relative abundances of clay-mineral fractions were determined using their basal reflections and the intensity factors of Moore and Reynolds (1989). Representative clay-abundant bulk samples were prepared for SEM-EDX analysis by adhering the fresh, broken surface of each whole-rock sample onto an aluminum sample holder using double-sided tape, and then coating the sample with a thin film (350 Å) of gold using a Giko ion coater. The DTA-TG curves were obtained using 10 mg of powdered clay sample in a Pt sample holder at an average heating rate of 10ºC/min with an alumina reference.

Chemical analyses of 18 whole-rock and six 2 μm fractions were carried out using inductively coupled plasma atomic emission spectroscopy (ICP-AES) for major and trace elements at Acme Analytical Laboratories, Ltd. (Vancouver, British Columbia, Canada). The detection limits for analyses were between 0.01 and 0.1 wt.% for major elements, and between 0.1 and 5 ppm for trace elements.

The enrichment and depletion of elements were estimated using the procedure of MacLean and Kranidiotis (1987). In those calculations, Zr was assumed to be the most immobile element based upon calculated correlation coefficients with other elements. All samples were grouped on the basis of degree of alteration (average result from each group), and the gains and losses of components were calculated using a starting mass of 100 g of average fresh anhydrous sample. The equation used in calculations can be written for SiO_2 (MacLean and Kranidiotis, 1987) as:

$$SiO_2\ (g/100\ g) = \frac{SiO_2\ (wt.\%)^{altered}_{rock}}{Zr\ (ppm)^{altered}_{rock}} \text{altered rock} \times Zr\ (ppm)^{fresh}_{rock}$$

Gain and loss of mass were determined by subtracting the calculated values from the concentrations of components in the least-altered samples, using the above formula.

Analyses of stable H and O isotopes were performed on four smectitefractions at Activation Laboratories, Ltd. (Actlabs, Ancaster, Ontario, Canada). The H-isotopic analyses, carried out using conventional isotope-ratio mass spectrometry, are reported in the familiar notation of per mil relative to the Vienna Standard Mean Ocean Water (V-SMOW) standard. The procedure described above was used to measure a δD value of −65‰ for the NSB-30 biotite standard. The O-isotopic analyses were performed using a Finnigan MAT Delta dual inlet isotope-ratio mass spectrometer, following the procedure of Clayton and Mayeda (1963). The data are reported in the standard delta notation as per **mil** deviations from V-SMOW. External reproducibility was ±0.19‰ (1σ), based on repeat analyses of the internal white crystal standard (WCS). The NBS 28 value was 9.61±0.10‰ (1σ).

GEOLOGICAL SETTING

The Eastern Pontides is one of the best preserved examples of a paleo-arc setting formed by subduction of the Tethyan ocean crust, which took place from the Jurassic to the Miocene period (Dixon and Pereira, 1974; Şengör and Yılmaz, 1981; Okay and Şahintürk, 1997). The Eastern Pontides straddle the North Anatolian transform fault, displaying three major volcanic cycles in the Jurassic, Upper Cretaceous, and Tertiary periods. Volcanic rocks of Jurassic age are transitional (Arslan *et al.*, 1997; Şen, 2007); those of the Upper Cretaceous are subalkaline; and Eocene−post Eocene volcanic rocks are alkaline and calcalkaline in character (Arslan *et al.*, 1997; Şen *et al.*, 1998; Arslan and Aslan, 2006; Arslan *et al.*, 2007; Temizel and Arslan, 2008). In the Late Cretaceous, the northern zone of the Eastern Pontides had very dense volcanic activity, mostly under submarine conditions, which led to the formation of shallow marine conditions and lagoons (Gedik, 2001, 2003).

In the region, bentonite, kaolinite, and illite developed in the alteration zones of the ore bodies (VMS, vein type, etc.) and by *in situ* alteration of Upper Cretaceous pyroclastics. Na and Ca-bentonite occurrences in Turkey, located mainly at Tirebolu (Giresun), Ünye-Fatsa (Ordu), Reşadiye (Tokat), and Kocaeli areas from east to west direction in Northwest and Northeast Anatolia, are generally formed within Late Cretaceous and Tertiary volcanics, or volcano-sedimentary rocks (Çoban and Ece 1999; Yalçın and Gümüşer, 2000; Uz and Bacak 2001; Abdioğlu, 2002; Uz *et al.*, 2003; Abdioğlu and Arslan, 2005; Arslan *et al.*, 2006). Some of these clay occurrences are now of economic interest.

The bentonite occurrences studied were of varying size in the Tirebolu area (Giresun, NE Turkey) and are distributed over ~70 km^2 (Figure 1). The basement of the study area is represented by the Late Cretaceous Çayırbağ formation, which consists of basalt and its pyroclastics. This formation is conformably overlain by the Tirebolu formation, consisting of trachyte, trachy-andesite, hyalo-trachyte, rhyodacite, dacite, their pyroclastics, and bentonites. The Tirebolu formation is overlain by marl, clayey limestone, and limestone units of the Kireçhane formation, which are outcrops of the study area. These units are overlain by Neogene basalt-andesite lava flow and dykes. All of these units are unconformably overlain by Quaternary alluvium materials (Figures 1, 2).

https://doi.org/10.1346/CCMN.2010.0580112 Published online by Cambridge University Press

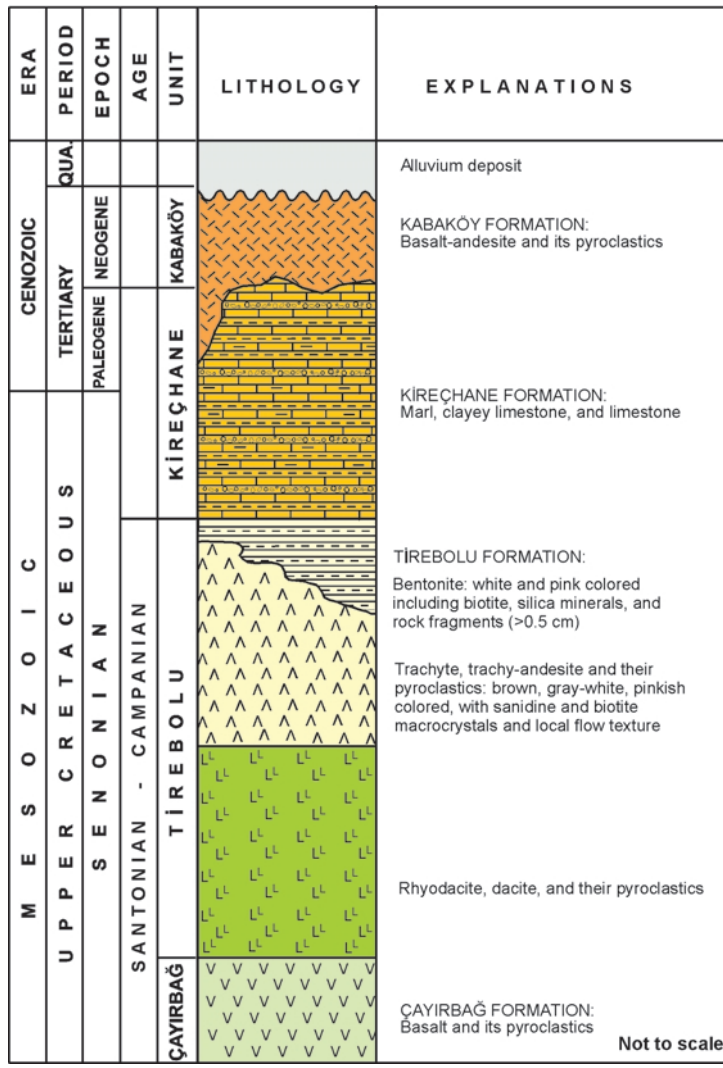

Figure 2. Simplified stratigraphic section of the study area indicating the vertical distribution of bentonite and volcanic rocks.

The bentonite in the Tirebolu formation, which is known as Tirebolu Bentonite, is a non-cemented clay bed ~5 m thick, exhibiting white, yellow, and pinkish colors and hard, soapy, and slippery characteristics. During dry periods, surface outcrops of the bentonite are easily distinguished by a popcorn-like texture. Pyrogenetic biotite, lithic fragments, and diagenetic siliceous minerals can even be seen with the naked eye in the bentonites. The lower and upper contacts of the bentonite grade into partly altered ignimbritic tuff and trachyte-trachyandesite flows.

RESULTS

Petrographical determinations

Volcanic rocks of the Tirebolu Formation within the study area generally consist of trachyte, trachyandesite, rhyolite, rhyodacite, and pyroclastic equivalents. Hyalotrachytes exhibit perlitic, snowflake, and spherulitic devitrification textures (Figure 3). In general, the pyroclastic rocks are composed of sanidine, plagioclase, titanomagnetite, scarce pyrite, hornblende, and apatite. The rocks show disequilibrium textures such as oscillatory zoning, sieve texture, and corrosion in plagioclase phenocrysts (Figure 3a–b), as well as breakdown and opaque hornblende, biotites, and devitrification of volcanic glass (Figure 3c–f). The pyroclastic rocks include crystal tuff, vitric crystal tuff, and ignimbrite. Crystal constituents in these pyroclastic rocks are sanidine, biotite, primary and secondary quartz, opaque minerals, clay minerals, and, rarely, plagioclase. Rock fragments are trachytic in composition. Ignimbrites contain crystals, glass shards, glassy pumice fragments, and, rarely, rock fragments. In most cases, eutaxitic texture with intense

https://doi.org/10.1346/CCMN.2010.0580112 Published online by Cambridge University Press

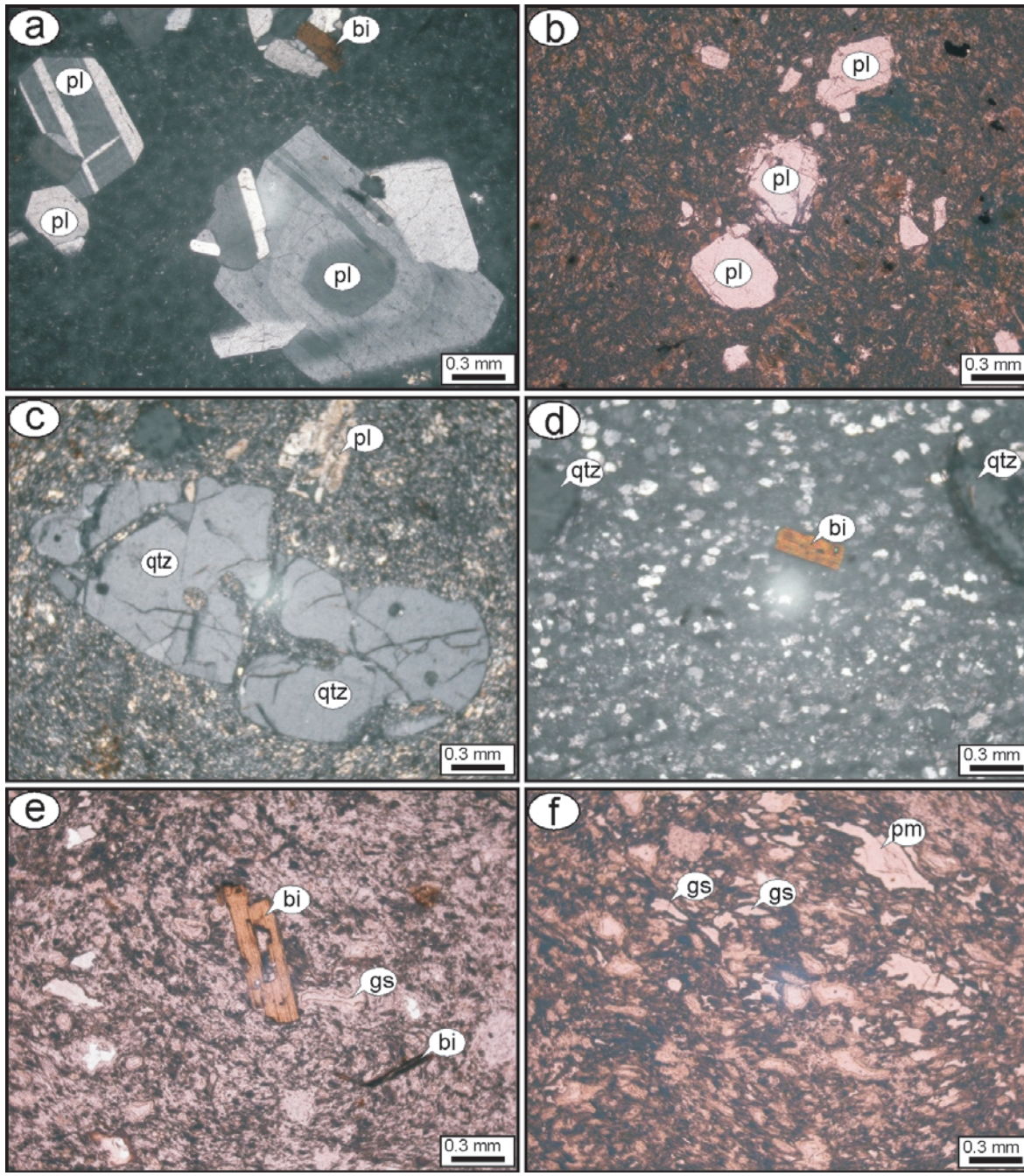

Figure 3. Optical photomicrographs of parent and surrounding volcanic rocks of bentonite: (a) trachyte exhibiting a hyalo-microlitic porphyritic texture (XPL); (b) vitric crystal tuff in trachyte composition (PPL); (c) embayed quartz crystals in argillitized groundmass of dacite (XPL); (d) dacite containing biotite phenocrysts and quartz microcrystals in groundmass formed by the devitrification of glass (XPL); and (e,f) vitric tuff in rhyodacite composition, containing abundant glass shards and pumice fragments (PPL). XPL: crossed nicols; PPL: plane-polarized light; pl: plagioclase; qtz: quartz; bi: biotite; gs: glass shards; pm: pumice.

welding, compaction, alignment of flattened glassy pumice fragments, and elongated-curved glass shards are characteristic. Some of the biotites exhibit deformation textures due to compaction of the rocks.

XRD

The XRD studies of bulk samples from several short profiles in the Tirebolu region revealed that smectite- and kaolinite-type alteration products are accompanied by

https://doi.org/10.1346/CCMN.2010.0580112 Published online by Cambridge University Press

feldspar (K-feldspar and plagioclase), quartz, and opal-CT, as well as amphibole and calcite in places (Table 1, Figure 4). Smectite is the prevalent clay mineral associated with abundant kaolinite in the TIR-2 sample and mordenite in the TIR-5, TIR-6, TIR-19B, TIR-25A, TIR-25B, TIR-25C, TIR-22B, and TIR-22C samples; in all samples smectite ± kaolinite ± mordenite ± illite coexist with feldspar and opal-CT + quartz. The smectite is determined by its reflections at 14.00−15.34 Å (Figure 4). These peaks expanded to ~17 Å following ethylene-glycol solvation, and collapsed to 9.87 Å upon heating to 350ºC. Additional heating to 550ºC caused further reduction in the sharpness and reflection of the peaks at 9.60 Å. The XRD patterns in Mg- and K-saturated samples were typical of a nearly pure smectite (Figure 5a), with an almost harmonic series of peaks. Mg-saturated samples gave a very strong 001 reflection at 14.50−14.80 Å in an air-dried state and 16.50−16.80 Å in an ethylene glycol-solvated state. K-saturation treatment collapsed smectite to 12.2−12.3 Å and heat treatment at temperatures up to 350ºC and 490ºC collapsed the smectite to 11.9 Å and 9.90 Å, respectively. Although the results indicate a pure smectite composition, the lack of strict harmonicity indicates possible interstratification effects of the layers with different thicknesses. The d_{060} values between 1.49 and 1.50 Å indicate dioctahedral smectite (Moore and Reynolds, 1989). The results of testing, based on the Greene-Kelley test, using Li-saturated samples which had been heated for 12 h and then solvated with ethylene glycol, indicated that the smectite has both montmorillonitic (9.28−9.74 Å) and beidellitic (16.36−17.06 Å) characteristics (Figure 5B). The test does not distinguish between all montmorillonites and beidellites, however. As much as 49% of the layer charge of montmorillonite may, therefore, have arisen from tetrahedral substitution, and even as little as 20% would have sufficed to retain expansibility and lead to an identification of beidellite (Buhmann *et al.*, 1985; Wilson, 1987).

Where present, kaolinite is characterized by well developed 7.18 Å, 3.57 Å, and 2.55 Å peaks indicating that it is a highly ordered kaolinite (Figure 4). These

Table 1. Mineralogical composition of the Tirebolu (Giresun) bentonites and surrounding volcanic rocks.

Sample	smc	kao	mrd	ill	fds	qtz	op-CT	amph	cal
TIR-2	+	+++			+	+	+		
TIR-3	++++				+				
TIR-4	+++			acc	++	+			
TIR-5	++++				acc	acc			
TIR-6	+		++		++	+	+		
TIR-9	+++		+	+	+	+			
TIR-10A	+++++			acc			acc		
TIR-10B	++++				acc	acc	+		
TIR-10C	+++			acc			+		
TIR-10D	+++						++		
TIR-11A	+++				acc	+			
TIR-11B	+++					+			
TIR-11D	++++					acc			
TIR-11E	++				++	+	acc		
TIR-11F	+++					acc	acc		
TIR-12	+++			acc	acc	+	+		
TIR-15	acc			acc		+	++		+
TIR-16A	+++			acc		acc	+		
TIR-16B	++			acc	acc	+	++		
TIR-17A	+++			acc	+		+		
TIR-17B	++++			acc			acc		
TIR-19B	++		+		+	+	+	acc	
TIR-21A	+++			acc		acc	++		
TIR-21B	++++								
TIR-22	acc				+	+	++	acc	
TIR-22B	+++		acc		+	acc	+		
TIR-22C	++++		acc		+	acc		acc	
TIR-25A	+++		+		+		+		
TIR-25B	++		+	acc	+		++		
TIR-25C	++		+	acc	+		++		
TIR-26C	++++		acc		acc		+		
TIR-26B	+++				acc	acc	++		
TIR-27	+++				acc	acc	acc		

smc: smectite, kao: kaolinite, ill: illite, mrd: mordenite, fds: feldspar, qtz: quartz, op: opal-CT, amph: amphibole, cal: calcite, +: relative abundance of mineral, acc: accessory.

https://doi.org/10.1346/CCMN.2010.0580112 Published online by Cambridge University Press

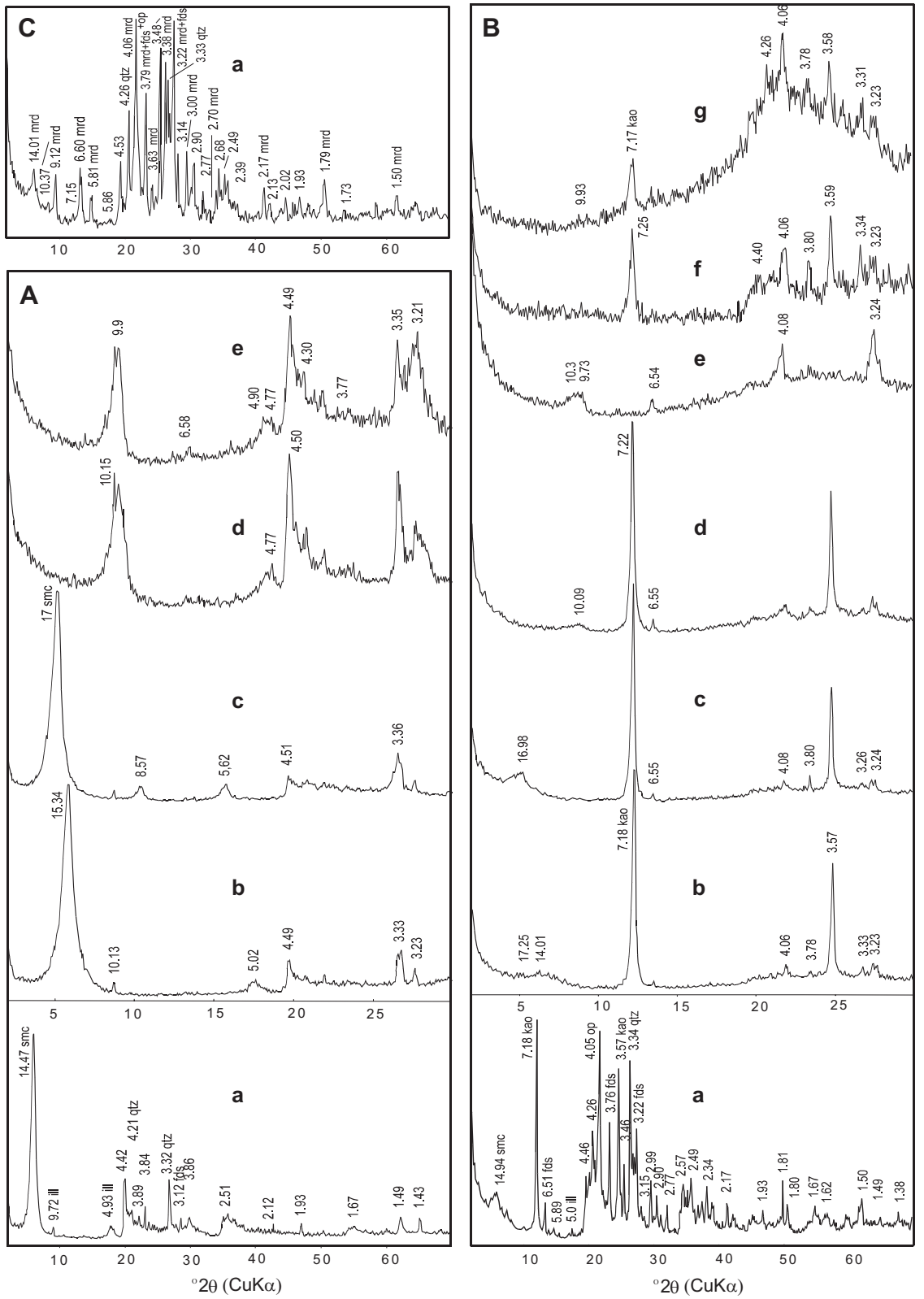

Figure 4. XRD patterns of Tirebolu bentonite samples (A) smectite (TIR-11D); (B) kaolinite (TIR-2); (C) mordenite (TIR-6) sample. a – powder; b – oriented; c – ethylene glycol solvated; d – heated to 350ºC; e – heated to 550ºC; f – strong K-acetate treatment; g – removal of K-acetate by washing and addition of ethylene glycol.

https://doi.org/10.1346/CCMN.2010.0580112 Published online by Cambridge University Press

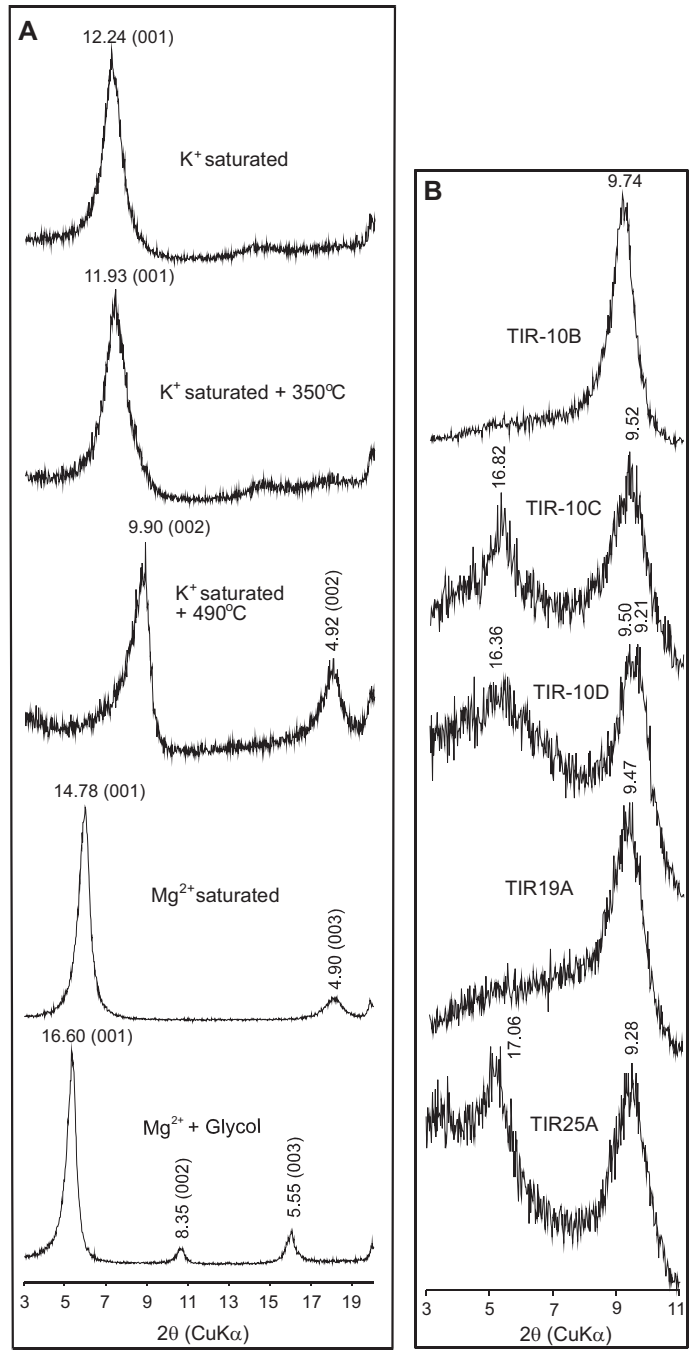

Figure 5. (A) XRD patterns of the oriented smectite fractions (TIR-10C) after Mg and K saturation, glycolation, and heat treatment. (B) XRD patterns of the oriented smectite fractions after Li saturation, heating for 12 h, and the addition of ethylene glycol.

peaks were not affected by ethylene-glycol treatment and heating to 350ºC, but collapsed following heating at 550ºC. The 7.18 Å peak of kaolinite was not affected by treatment with K-acetate solvation, or by washing with water and the addition of ethylene glycol, suggesting kaolinite rather than halloysite, as reported by Wilson (1987), Churchman and Gilkes, (1989), Churchman (1990), and Arslan *et al.* (2006).

SEM-EDX determinations

The SEM studies revealed that smectite developed authigenically as 'cornflakes' in dissolution voids of altered glassy pyroclastic material (Figure 6a–b). These flakes are ~1.5 μm in diameter. In addition, mordenite developed as needle-like structures; either irregularly as a bunch of needles edged mostly by relicts of devitrified volcanic glass, or as needle mesh away from the

https://doi.org/10.1346/CCMN.2010.0580112 Published online by Cambridge University Press

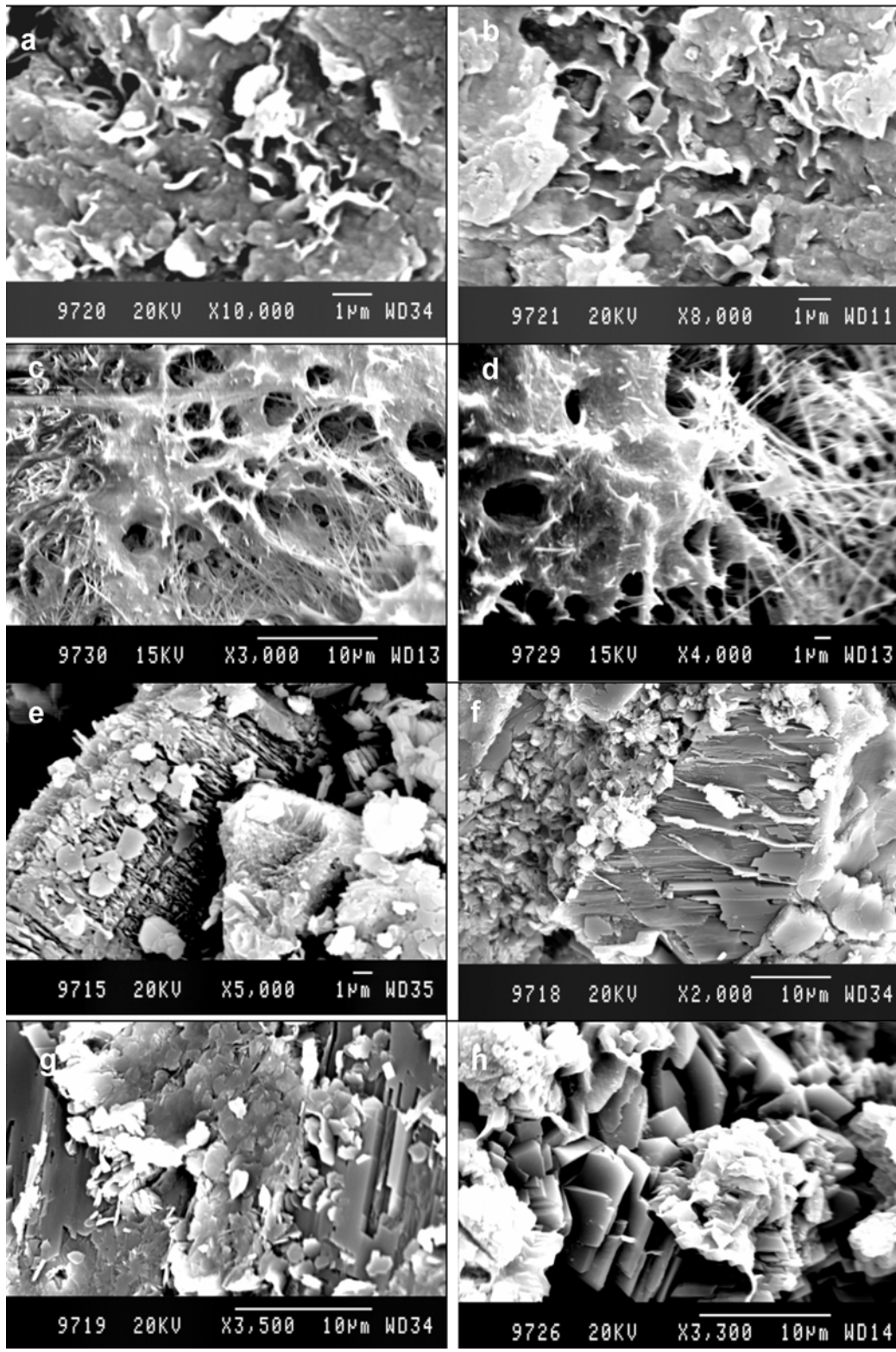

Figure 6. SEM images: (a, b) smectite flakes developed as cement in dissolution voids of volcanic glass (TIR-10B); (c, d) Development of mordenite needles in intimate association with devitrified volcanic glass (TIR-6); (e) view of vermiform kaolinite (TIR-2); (f) development of kaolinite crystals in contact with resorbed feldspar crystals (TIR-2); and (g, h) kaolinite crystals on resorbed feldspar (TIR-2, TIR-6).

https://doi.org/10.1346/CCMN.2010.0580112 Published online by Cambridge University Press

devitrified volcanic glass (Figure 6c–d). Kaolinite occurs either in a vermiform shape, when developed independently, or as irregular plates when developed in fractures and subparallel to resorbed feldspar (Figure 6e–f). Resorbed feldspar has thin to thick parallel platy forms (Figure 6g–h).

DTA-TG

The DTA-TG curves of smectite sample TIR-17B indicate that dehydration occurred in three stages (Figure 7a). The first strong asymmetric endothermic peak occurred at temperatures between 20 and 250ºC (mean: 152ºC; weight loss: 15%), the second medium peak occurred at temperatures of 620 to 725ºC (mean: 678ºC; weight loss: 3.5%), and the last and smallest peak occurred at temperatures between 837 and 915ºC (mean 883ºC, weight loss: 0.5%). Thermally, the constitution was gradually lost and the structure finally collapsed at 1032ºC. The first endothermic peak represents the elimination of hygroscopic and zeolitic water, and the second and third endothermic peaks are due to dehydroxylation of the constitution water of the structure.

The trace smectite-bearing kaolinite sample, TIR-2, exhibits two endothermic peaks (Figure 7b), the first below 144ºC (mean: 104ºC; weight loss: 2.8%) and the second large symmetric endothermic peak at 554ºC (weight loss: 3.7%). The first endothermic peak is attributed to the loss of zeolitic and bound water of trace smectite accompanying the kaolinite in this sample. This low-temperature endothermic peak is not characterized as resulting from the presence of halloysite, based on K-acetate treatment and XRD analyses. The second symmetric, endothermic peak at 554ºC is due primarily to dehydration of ordered kaolinite crystals, similar to that which was reported by MacKenzie (1957) and Paterson and Swaffield (1987). The structure of kaolinite collapsed at the 988ºC exothermic peak.

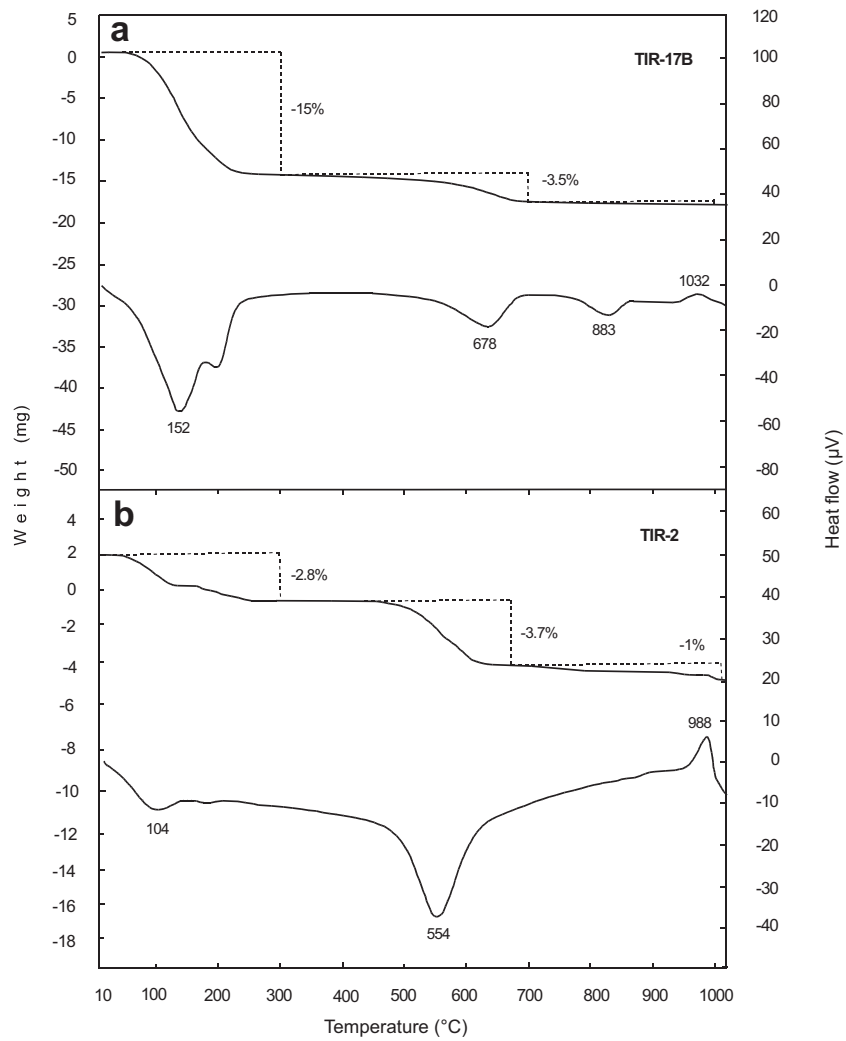

Figure 7. DTA-TG curves for: (a) smectite-dominated sample (TIR-17B); (b) a smectite-bearing kaolinite sample (TIR-2).

https://doi.org/10.1346/CCMN.2010.0580112 Published online by Cambridge University Press

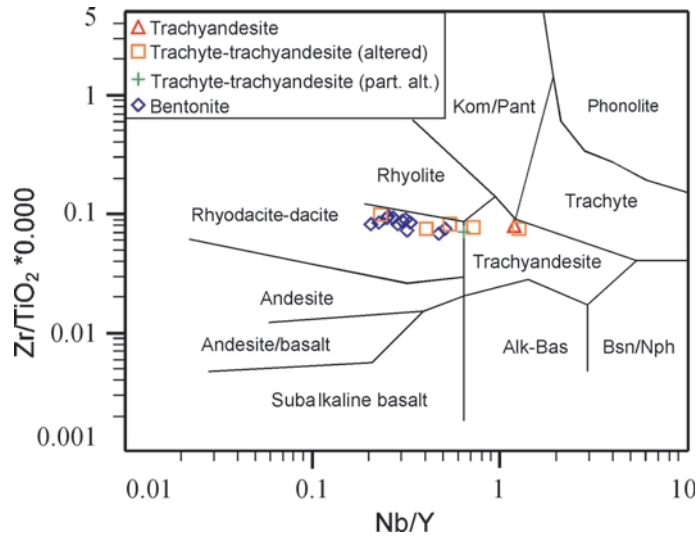

Figure 8. Petrochemical discrimination plot of the bentonite and surrounding volcanic samples of the Tirebolu area, using an Nb/Y-Zr/TiO_2 immobile element diagram of Winchester and Floyd (1977).

GEOCHEMISTRY

Parent rock of the bentonite

When the Tirebolu area samples were plotted on a Winchester and Floyd (1977) immobile-element diagram (Zr/TiO_2, Nb/Y), the bentonite appeared in the rhyodacite/dacite field, but partly altered and unaltered samples plotted in both the trachyandesite and rhyodacite/dacite fields (Figure 8). Furthermore, petrographic investigation of these pyroclastic rocks indicated a trachyandesitic to rhyodacitic composition. In addition, partly altered rocks plotted in and near the trachyandesite field, while bentonite samples plotted in the rhyodacite/dacite field, which led to the consideration that Nb may have leached during alteration processes.

The results of 18 bentonite whole-rock chemical analyses for major and trace elements showed that the samples consisted of SiO_2 (55.3–72.46 wt.%), Al_2O_3 (10.45–17.08 wt.%), Fe_2O_3 (0.83–2.24 wt.%), MgO (0.82–4.17 wt.%), and TiO_2 (0.07–0.29 wt.%). Loss on ignition was 2.7–16.7 wt.% (Table 2). The alkali content of the bentonites was much smaller than fresh-rock composition, indicating a major loss of alkalis during alteration, as might be expected (*e.g.* Senkayi *et al.*, 1984; Shiraki *et al.*, 1987; Altaner and Grim, 1990; Christidis and Scott, 1997). The relatively large K_2O and Na_2O contents of some of the bentonite samples reflect the presence of authigenic K-feldspar and mordenite, respectively. The MgO content of all bentonites is considerably greater than that of the fresh-rock composition, implying that Mg has been taken up during the alteration of the parent pyroclastics, or that some small-scale local redistribution of Mg may have taken place. Such an environment is similar to that at Milos and Kimolos islands where sea water has been shown to be the source of most of the Mg (Christidis *et al.*, 1995; Christidis and Scott, 1997). Mg uptake is a common consequence of alteration of volcanic glass (Mottl and Holland, 1978; Shiraki *et al.*, 1987). All samples had a similar trace-element composition that was compatible with their precursor material.

Incompatible element concentrations of both pyroclastic and bentonitic samples were normalized to N-type Mid Ocean Ridge Basalt (MORB) in order to collect information about the source of the parent rock of the bentonites (Figure 9). Bentonite samples have small Sr, Ti, P, relatively small Ba, and large K, Rb, and Th contents. Generally, the incompatible element composition of the bentonites is similar to the surrounding volcanic rocks, suggesting that the incompatible elements were generally immobile during alteration processes.

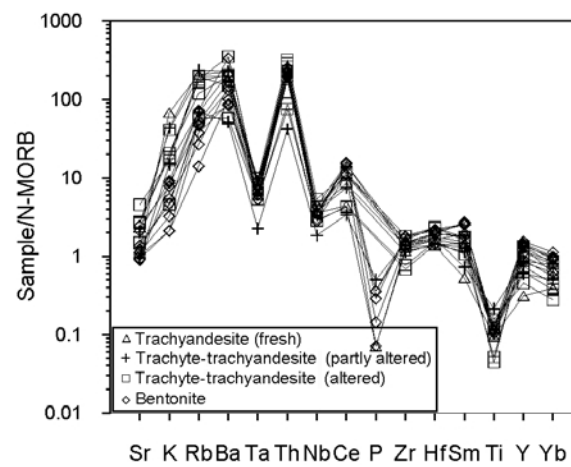

Figure 9. N-type MORB normalized spider diagram of the bentonite and surrounding volcanic samples of the Tirebolu area. Normalizing values are from Sun and McDonough (1989).

https://doi.org/10.1346/CCMN.2010.0580112 Published online by Cambridge University Press

Table 2. Major oxide (wt.%) and trace element (ppm) concentrations of the bentonite and surrounding rock samples from the Tirebolu (Giresun) area.

	Bentonite samples								Altered rock samples							Partly altered rock		Fresh rock
	TIR-10A	TIR-10B	TIR-10C	TIR-10D	TIR-21B	TIR-26A	TIR-26B	TIR-27	TIR-3	TIR-5	TIR-9	TIR-19A	TIR-19B	TIR-25A	TIR-25B	TIR-8	TIR-13	TIR-1
SiO_2	66.14	63.97	71.16	72.46	73.24	64.37	67.94	70.82	58.73	55.3	59.79	60.08	67.25	67.28	71.68	69.15	72.74	76.04
Al_2O_3	13.67	12.62	12.01	11.78	10.45	14.63	13.55	11.66	15.2	17.08	14.17	16.44	13.09	13.26	10.92	11.71	13.67	11.32
Fe_2O_3*	1.41	1.29	1.16	1.19	0.85	0.92	0.83	1	1.45	1.33	1.68	1.31	0.95	1.18	0.9	1.15	2.24	0.68
MgO	3.4	2.94	2.92	2.9	2.6	3.08	2.92	2.48	2.56	2.01	2.42	4.17	2.41	2.03	0.82	0.98	2.35	0.2
CaO	1.73	1.46	1.11	0.95	0.84	0.9	0.71	0.79	2.15	1.94	1.82	2.58	2.34	2.34	2.41	1.37	0.29	0.82
Na_2O	0.41	0.38	0.23	0.2	0.18	0.28	0.24	0.07	1.18	0.85	1.38	0.53	1.09	0.89	1.2	1.49	4.03	1.7
K_2O	0.7	0.82	0.42	0.29	0.19	0.49	0.19	0.77	1.64	3.69	1.85	0.41	1.86	0.82	1.5	3.88	1.33	6.11
TiO_2	0.17	0.17	0.14	0.14	0.16	0.15	0.15	0.14	0.18	0.21	0.17	0.07	0.06	0.17	0.14	0.14	0.29	0.13
P_2O_5	0.05	0.04	0.02	0.05	0.01	<0.01	<0.01	<0.01	<0.01	<0.01	<0.01	<0.01	<0.01	<0.01	<0.01	<0.01	0.07	0.01
MnO	0.07	0.05	0.04	0.04	0.02	0.09	0.01	0.05	0.24	0.44	0.24	0.2	0.07	0.3	0.07	0.07	0.07	0.02
Cr_2O_3	0.004	0.003	0.002	0.004	0.001	<0.001	<0.001	0.005	0.002	0.001	0.002	<0.001	<0.001	0.001	0.004	0.005	0.004	0.005
LOI	12	15.9	10.3	9.8	11.3	15	12.7	11.9	16.7	16.4	16.2	14.4	10.6	11.6	10	9.4	2.7	2.7
TOT/C	0.01	0.02	0.02	0.01	0.02	0.04	0.03	0.03	0.01	0.03	0.03	0.02	0.01	<0.01	<0.01	0.01	0.03	0.01
TOT/S	0.03	0.04	0.02	0.01	0.01	0.01	<0.01	0.02	0.01	0.01	0.01	0.01	0.01	0.01	0.01	<0.01	0.02	0.01
SUM	99.91	99.87	99.62	99.86	99.9	100.01	99.32	99.77	100.17	99.36	99.86	100.23	99.86	100.03	99.89	99.51	99.82	99.9
Ba	1354	2117	1058	528	554	916	628	828	1222	940	1295	363	1250	1372	2210	1438	323	1418
Sc	3	3	3	5	4	3	4	2	5	4	4	4	4	5	3	3	8	4
Co	1.1	1.8	2.9	1.9	2.2	0.7	0.6	<0.5	1.7	2	1.3	0.6	0.5	0.5	<0.5	0.6	2.5	<0.5
Cs	4	3.9	3.8	4	3.9	3.6	3.8	7.5	10.6	1.5	7.1	3.5	4.5	4.4	8.2	6.1	0.1	1.2
Ga	14.5	13.5	11.9	11.8	9.8	14.6	11.5	10.1	16.6	18.8	15.5	17.2	12.8	17.2	10.3	9.9	12.9	13
Hf	4.5	4.3	3.9	4	2.9	4	3.3	3.3	4.8	4.7	4	3.1	2.9	3.5	3.6	2.9	3.4	2.8
Nb	10	8.5	7	8	8.6	8.5	8	6.5	10	12.5	8.7	6.6	6.7	9.7	8.9	8.6	4.3	8.3
Rb	38.2	40.5	29.4	27.3	21	14.9	7.8	26.1	111	108.9	95	32.1	66.8	53.7	100.9	132.6	38.7	116.4
Sr	221.1	189.2	123.5	100.8	92.8	111.2	83.9	80.4	248	235.7	242	135.3	239.6	259.5	408	183.2	85.2	112.7
Ta	1.2	1	0.8	0.9	0.7	1.1	0.8	0.7	1.1	1.3	1	0.7	0.7	1.1	1	0.8	0.3	0.8
Th	30	27.9	24.8	27.3	23.6	26.3	30.8	23	34.9	38.6	31.4	10.7	9	29.8	23.4	24.3	5	21.2
U	5.9	7	6.5	4	6	2	2.6	2.1	1.8	3.2	3.1	1.4	1.6	5.3	2.6	3.6	0.9	8.4
V	7	7	<5	<5	10	5	<5	<5	10	9	7	<5	<5	6	5	6	28	<5
W	2	2.6	1.9	0.9	4.2	2.1	2.1	1.7	0.6	2.1	0.8	0.3	0.6	4.2	5.5	1.2	0.9	2.6
Zr	128.8	133.1	101.7	111	93.3	111.9	92.7	100.4	118.3	134.2	108.6	56.9	50.1	117.5	98.7	83.2	111.2	87.2
Y	31.9	33.8	30.6	29.7	18.3	28.2	24.6	19.6	13.9	9.9	21.4	25.6	29.1	34.1	16.3	13.2	18.9	6.9
Cu	4.7	1.4	4.1	2.6	1.2	1.5	4.7	1.7	3.1	3.8	4.2	8.8	4.2	2.2	1.4	3.8	2.8	3.8
Sn	2	1	2	2	1	2	2	1	2	2	2	4	3	2	2	1	1	1
Pb	11.6	9.9	11.1	14.5	17.6	18.6	18.2	17.3	12.1	63.2	42.9	31	31.5	17	5.8	9.5	4.4	3.5
Zn	12	10	11	13	14	7	10	6	12	25	26	13	12	18	11	16	59	7
Ni	1.9	1.8	1.6	1.7	2	0.9	1.4	1	2	1.4	2.5	1.1	0.7	0.4	0.1	1.1	1.5	1.5

All Fe as Fe_2O_3; LOI is loss on ignition. TOT/C: total carbon. TOT/S: total sulfur

Rare earth element (*REE*) contents of the parent rock and bentonite samples (Table 3) were normalized to chondrite composition (Sun and McDonough, 1989), exhibiting varying degrees of Eu anomaly (Figure 10). The bentonite samples have similar *REE* patterns to each other, but differences in Eu anomalies (Eu_N/Eu^* = 0.18−0.75) indicating bentonite formation from different pyroclastics. Smectite-rich clay samples exhibit light *REE* enrichment. The absence of a negative Ce anomaly also suggests that argillization took place under suboxic or anoxic conditions (Jeans *et al.*, 2000).

Mass-change calculations

During rock-alteration processes some elements are mobile while others are immobile and become enriched in the rocks during alteration processes. In order to determine the details of this enrichment and depletion, the method of MacLean and Kranidiotis (1987) was used. For the calculations, Zr was accepted as the most immobile element, based on its large correlation coefficients with other immobile elements (Table 4). All samples were grouped according to their clay content. The gain and loss of components were calculated using a starting mass of anhydrous trachyandesite (sample TIR-1).

Based on major-oxide histograms (Figure 11), Si is lost in almost all samples. Al behaves differently in the different samples according to their degree of alteration. In partly altered and altered samples, Al is enriched, as an indication of kaolinite in these samples; it is nearly immobile in the others. The Na is enriched at the beginning of the alteration and then it is depleted. This is also compatible with mineralogical data; the partly altered rock samples contain more mordenite than the others because the formation of mordenite requires Na leaching due to its high Na content. Ca is slightly

Table 3. Rare earth element (ppm) concentrations of the bentonite and surrounding rock samples from the Tirebolu (Giresun) area.

	Fresh rock	Bentonite samples							
	TIR-1	TIR-10A	TIR-10B	TIR-10C	TIR-10D	TIR-21B	TIR-26A	TIR-26B	TIR-27
La	21.00	68.50	63.20	66.00	61.20	45.80	64.40	59.20	53.60
Ce	33.10	114.40	103.20	117.10	112.30	82.20	111.90	110.90	82.10
Pr	3.02	11.57	11.12	12.29	11.34	7.48	10.53	10.57	8.12
Nd	9.40	38.40	36.80	41.80	37.90	22.80	32.40	33.40	24.30
Sm	1.40	6.70	6.60	7.10	6.90	3.40	4.70	5.10	3.70
Eu	0.72	1.34	1.36	1.41	1.28	0.66	1.05	1.05	0.69
Gd	0.91	5.57	5.19	5.76	4.97	2.56	4.17	3.9	2.83
Tb	0.16	0.86	0.78	0.91	0.89	0.48	0.62	0.64	0.43
Dy	0.98	4.97	4.70	5.16	4.63	2.64	3.92	3.66	2.68
Ho	0.25	1.00	1.08	0.97	0.99	0.57	0.85	0.76	0.53
Er	0.72	2.78	3.19	2.78	3.02	1.65	2.16	2.43	1.55
Tm	0.17	0.42	0.48	0.41	0.43	0.26	0.35	0.34	0.25
Yb	1.19	2.99	3.40	2.80	2.94	1.88	1.86	2.39	1.68
Lu	0.20	0.48	0.54	0.47	0.47	0.31	0.3	0.38	0.29
(Eu_N/Eu^*)	1.83	0.65	0.69	0.65	0.64	0.66	0.71	0.69	0.63
		Altered rock samples						Partly altered rock	
Element	TIR-3	TIR-5	TIR-9	TIR-19A	TIR-19B	TIR-25A	TIR-25B	TIR-8	TIR-13
La	49.9	53.70	50.20	13.40	12.70	55.70	41.50	31.70	10.10
Ce	82.8	86.70	88.90	32.60	31.70	97.70	63.20	56.10	25.30
Pr	8.25	8.42	8.39	3.51	3.61	10.23	7.40	5.49	2.35
Nd	28.10	26.60	27.5	11.50	13.10	33.70	23.40	17.60	8.80
Sm	4.50	4.20	4.60	2.80	3.80	6.00	4.00	3.00	1.90
Eu	0.82	0.86	0.88	0.36	0.47	1.01	0.73	0.60	0.50
Gd	3.07	2.57	3.40	2.72	3.82	4.95	3.45	2.06	2.17
Tb	0.45	0.41	0.60	0.58	0.72	0.89	0.47	0.35	0.41
Dy	2.44	2.01	3.27	3.34	4.23	4.60	2.67	1.93	2.73
Ho	0.47	0.32	0.68	0.78	0.90	1.02	0.51	0.45	0.64
Er	1.13	0.80	1.83	2.41	2.61	2.90	1.34	1.31	2.04
Tm	0.17	0.12	0.29	0.36	0.37	0.43	0.20	0.23	0.31
Yb	1.14	0.85	2.08	2.63	2.49	3.03	1.36	1.53	2.39
Lu	0.21	0.19	0.34	0.38	0.39	0.46	0.21	0.27	0.41
(Eu_N/Eu^*)	0.64	0.74	0.65	0.18	0.37	0.55	0.59	0.70	0.75

$Eu^* = (Sm_N + Gd_N)/2$

https://doi.org/10.1346/CCMN.2010.0580112 Published online by Cambridge University Press

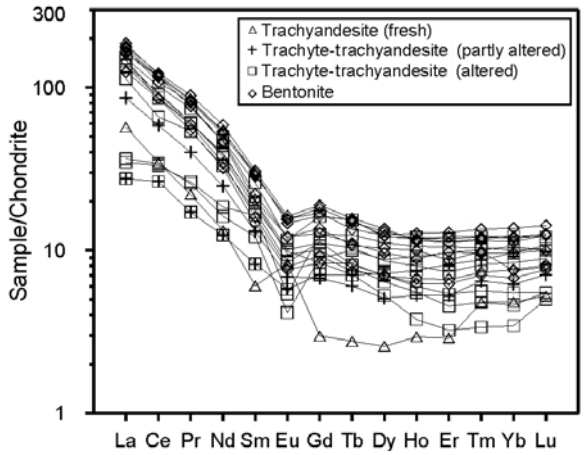

Figure 10. Chondrite-normalized *REE* patterns of the bentonite and surrounding volcanic samples of the Tirebolu area, showing enrichment and depletion of *REE* during the alteration processes. Normalizing values are from Taylor and McLennan (1985).

depleted and then enriched. Depletion and enrichment of Ca and Mg can be attributed to the formation of Ca-smectite and rare calcite. Mg is enriched in almost all the samples, while K is depleted. The Mg content can increase by up to 15 times during the conversion of rhyolite to bentonite (Zielinski, 1982). The bentonite and altered rock samples studied have greater Mg contents than the fresh-rock composition. The calculated gains in Mg, therefore, might indicate a circulation between seawater and the precursor material of bentonites during and/or after the alteration period (Fisher and Schmincke, 1984). The gain and loss of Ba and Sr can be related to the breakdown of feldspar minerals and volcanic glass shards, and then leaching. In addition, the loss of Rb may result in the corrosion of biotites (Figure 11).

Table 4. Correlation coefficients of Al, Ti, Hf, Nb, Zr, and Y for the volcanic and bentonite samples of the Tirebolu (Giresun) area. The bold entries are meaningful values at $p < 0.0500$.

	Al	Ti	Hf	Nb	Zr	Y
Al	1.00	0.14	**0.49**	0.29	0.15	0.01
Ti	0.14	1.00	0.41	0.09	**0.73**	−0.21
Hf	**0.49**	0.41	1.00	0.57	**0.80**	0.16
Nb	0.29	0.09	**0.57**	1.00	**0.52**	−0.20
Zr	0.15	**0.73**	0.80	0.52	1.00	0.09
Y	0.01	-0.21	0.16	-0.20	0.09	1.00

Mineral chemistry

The chemical composition of the six purified smectite samples (Table 5) shows that large SiO_2 values of the samples are due to the presence of free silica phases,

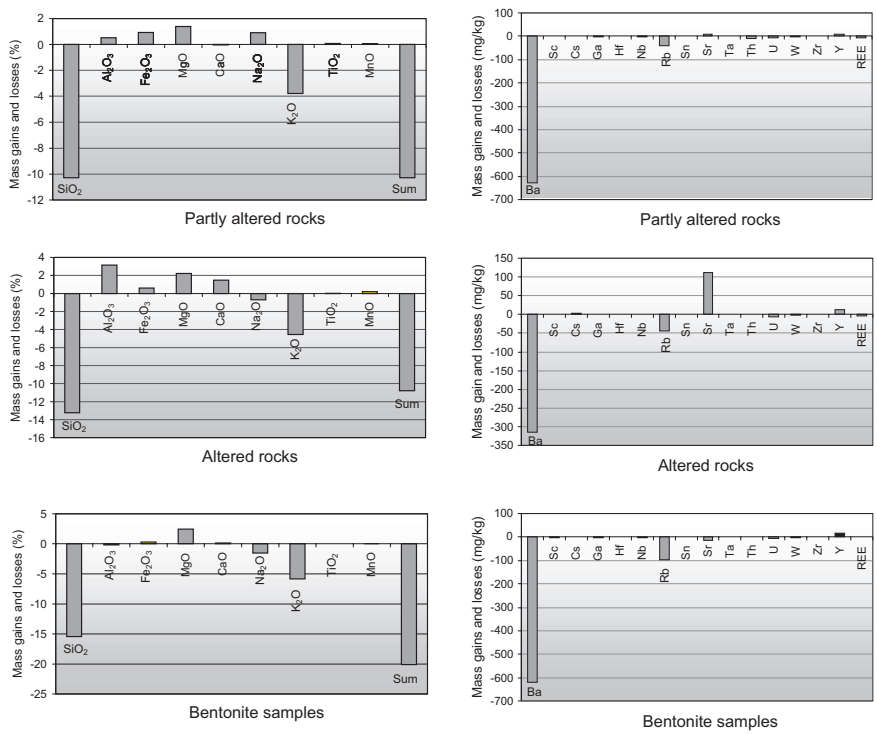

Figure 11. Mass balance change of the major oxides (g) and of the trace elements (ppm) for the Tirebolu area bentonite and surrounding rock samples.

https://doi.org/10.1346/CCMN.2010.0580112 Published online by Cambridge University Press

Table 5. Exchangeable cations, CEC, and pH value of smectite-rich bentonite samples from the Tirebolu (Giresun) area.

	TIR-10B	TIR-10D	TIR-19A	TIR-10C	TIR-25A
cmol(+)/kg					
Ca	34.05	24.08	73.42	29.57	49.44
Na	1.45	0.35	2.43	0.66	9.27
K	0.90	0.82	0.78	0.73	6.56
Mg	15.58	13.34	13.26	14.61	13.61
Al	–	17.33	–	9.72	–
Ca+Na+K+Mg+Al	51.99	55.93	89.89	55.30	78.88
CEC	58.64	65.42	94.26	64.32	87.68
pH	5.27	4.83	6.04	4.99	6.21

such as opal-CT and quartz. In the clay fractions, the Al_2O_3 content of the samples is small (10.12–12.23 wt.%). In the analysis, the total Fe_2O_3 values were 0.81–1.34 wt.%. This iron must be used in the octahedral site. Moreover, Na_2O is <0.1 wt% because clay minerals in the samples are generally Ca-smectite. The MgO content, occupying part of the octahedral sheet and interlayer space of the samples, ranges from 3.0 to 3.4 wt%. According to chemical analysis based on clay fractions, Si and ^{IV}Al are tetrahedral, while ^{VI}Al, Mg, Fe, Ti, and, rarely, Mn are octahedral. Ca, Mg, Na, and K are interlayer cations, along with Al in some samples.

The amount of exchangeable cations, cation exchange capacity (CEC), and pH value of six bentonite samples (Table 6) revealed the samples to be smectite, which is generally Ca- and Mg-saturated, with the main interlayer cation being Ca (29.57–73.42 cmol(+)/kg). The interlayer Na value fluctuates between 0.35 and 9.27 cmol(+)/kg. The samples generally contain a small amount of K, 0.70–0.93 cmol(+)/kg, except TIR-25A, which contains 6.56 cmol(+)/kg. Mg values of all the samples are similar to each other (13.26–15.58 cmol(+)/kg). Uno and Takeshi (1979) showed that smectite from weathered bentonite deposits were characterized by the presence of Mg, as well as H, in the interlayer position. The enrichment of Mg in smectite could be attributed not only to seawater, but also to the circulation of ground water. Furthermore, two samples (TIR-10D and TIR-10C) contain exchangeable Al. The pH values of the samples are between 4.83 and 6.21. The low pH value of two samples (TIR-10D and TIR-10C) is attributed to exchangeable Al.

Montmorillonite may be expected to form from solutions high in Si, Al, and Mg. Beidellite crystallizes from such solutions only if the pH is 6.7, and if exchangeable Al is present (Van Ranst, 1998). This is also consistent with these two samples. Both samples show a beidellitic character in the Li-saturated state, and contain exchangeable Al. The average CEC of smectites is accepted as 110 cmol(+)/kg. The CEC values of the smectites studied here, however, are less than this value, possibly due to the K and Fe content. Increases in the K_2O content decrease the CEC (Righi and Meunier, 1995).

Table 6. Chemical composition (wt.%) of the smectite fractions of bentonite samples from the Tirebolu (Giresun) area.

	TIR-10B	TIR-10C	TIR-10D	TIR-21B	TIR-26D	TIR-27
SiO_2	62.92	66.33	66.46	67.66	60.5	66.87
Al_2O_3	12.23	11.25	11.1	10.12	13.4	10.96
Fe_2O_3*	1.34	1.07	1.11	0.81	0.89	1.00
MgO	3.12	2.79	2.88	2.59	3.00	2.52
CaO	1.27	0.91	0.77	0.67	0.64	0.71
Na_2O	0.09	0.06	0.03	0.04	0.06	0.02
K_2O	0.54	0.36	0.21	0.18	0.45	0.53
TiO_2	0.16	0.12	0.12	0.15	0.15	0.13
P_2O_5	0.04	0.04	0.04	0.03	0.02	0.02
MnO	0.05	0.04	0.04	0.02	0.08	0.05
Cr_2O_3	0.001	0.003	<0.001	<0.001	<0.001	0.003
LOI	18.10	16.90	17.10	17.60	20.60	16.90
SUM	99.99	99.95	99.92	99.93	99.85	99.8

All Fe as Fe_2O_3
LOI is loss on ignition.

https://doi.org/10.1346/CCMN.2010.0580112 Published online by Cambridge University Press

Table 7. O- and H-isotopic compositions of the smectites from the bentonite samples of the Tirebolu (Giresun) area.

Sample	TIR-26A	TIR-26B	TIR-27	TIR-11C
$\delta^{18}O_{V\text{-}SMOW}$ (‰)	28	27.3	27.1	25.2
$\delta D_{V\text{-}SMOW}$ (‰)	−131	−122	−114	−120
Water content (wt.%)	6.3	6.3	6.4	8.2

Stable-isotope geochemistry of smectites

The O- and H-isotopic composition of smectites from the Tirebolu bentonite show narrow ranges from +25.2‰ to +28‰ and −114‰ to −131‰, respectively (Table 7). All data points from the smectite studied plot away from the smectite (SM) line representing the isotopic composition of smectites in equilibrium with meteoric water at 20ºC, but near the montmorillonite (Ml) field represented by the isotopic composition of Archidona montmorillonite (Figure 12). Sheppard *et al.* (1969) showed that hypogene clays and supergene clays, equilibrated at surface temperatures, can be distinguished from each other because the isotopic composition of hypogene clays plots closer to the meteoric water line. The isotopic composition of the smectites studied is also comparable with those of smectites formed as a result of the alteration of volcanic ash deposited during the Late Cretaceous (Elzea, 1990) (Figure 12). The results reveal that the Tirebolu smectite studied may have been formed at low temperature by normal Cretaceous ocean water, possibly with mixing of large volumes of fresh water.

To obtain information about the formation conditions of the minerals from their isotopic data, the minerals must retain the isotopic composition that they acquired during their formation (Faure and Mensing, 2004). The narrow isotopic ranges of the Tirebolu smectites may imply insignificant post-formation isotopic change. Isotopic fractionations of clay minerals at surface temperatures are extremely slow (Savin and Lee, 1988). All the isotopic compositions of the smectites studied were largely intact after their formation. The isotopic composition of fluid can be calculated theoretically at several temperatures ranging from 10 to 80ºC (Figure 13), following the fractionation equations.

As the precursor volcanic rocks of the Tirebolu bentonites formed in the shallow marine environment of the Pontide arc setting during the Upper Cretaceous, they can be used to obtain an estimate of the Cretaceous seawater isotopic composition. The effect of alteration of these values can be seen by plotting the Cretaceous seawater values together with the present-day isotopic composition of the Black Sea water and the values of meteoric water (Figure 13a,b). Estimates of $\delta^{18}O$ values for normal Cretaceous seawater range from −0.5‰ (Craig and Gordon, 1965; Savin *et al.*, 1975) to −1.0‰ (Shackleton and Kennett, 1975). Present-day $\delta^{18}O$ and δD isotopic compositions of the Black Sea are −3‰ and −25‰, respectively (Balderer, 1999), and the present-day ground water (meteoric waters) ranges from −12.2‰ to −13.73‰ for $\delta^{18}O$ and from −90.15‰ to −102‰ for δD (Gültekin, 1999). The ambient water responsible for smectite formation may have been seawater and meteoric water. If the components had an active role in the formation of smectites, the calculated isotopic composition of the ambient fluid would be between these two extremes. The isotopic composition of the present-day seawater and meteoric water may be different from those of the water eons ago, but when taking into account climatic variation in the region, these differences would be small.

In addition to groundwater and seawater, another type of water, magmatic water, was probable, which might have been present during the eruption and subsequent cooling (alteration) of the Tirebolu volcanic rocks. The O- and H-isotope compositions of the magmatic water

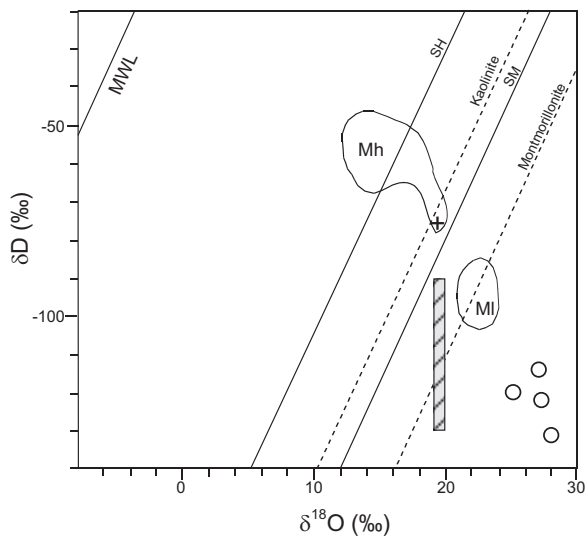

Figure 12. δD *vs.* $\delta^{18}O$ plot showing the isotopic composition of the smectites from the Tirebolu area. MWL: meteoric water line; the lines for kaolinite and montmorillonite are from Savin and Epstein (1970). SH: the supergene/hypogene line of Sheppard *et al.* (1969). SM: smectite line representing the isotopic composition of smectite in equilibrium with meteoric waters at 20ºC. Mh and Ml: isotopic compositional ranges of high-temperature and low-temperature montmorillonites, respectively. Black Sea: the isotopic composition of the present-day seawater (Balderer, 1999). The shaded area represents average Clay Spur Wyoming bentonite (Elzea, 1990) and the cross indicates non-marine bentonite from Chambers, Arizona (Savin and Epstein, 1970).

https://doi.org/10.1346/CCMN.2010.0580112 Published online by Cambridge University Press

have been calculated theoretically to range from +5.5‰ to +9.5‰ and from −80‰ to −40‰, respectively (Sheppard *et al.*, 1969).

The smectites studied were probably formed in a mixture of sea water and some meteoric water (Figure 13). Magmatic water can, however, mix with surface water and create hydrothermal-alteration conditions. If this were the case, the O-isotope composition of the samples would be very close to or slightly larger than those of the surface water (Yui and Chang, 1999). Such a situation would reduce the possible effect of magmatic water on the formation of the smectites studied.

In order make these assumptions reliable, the water/rock (w/r) ratio must be high in the system at the time of alteration. If the water/rock ratio were small, the $\delta^{18}O$ value would show little difference from the initial $\delta^{18}O$ of the precursor material. Water/rock ratio calculations were based on equations proposed by Ohmoto (1986) (equation 1). In the equation, $\delta^{18}O_{rock}^{initial}$ was accepted to be 6.5±1‰, which is a generally accepted value of basaltic and andesitic rocks (Taylor, 1979). As feldspar is considered the best mineral to indicate the isotopic composition of water, $\delta^{18}O_{rock}^{initial}$ was calculated at equilibrium temperatures ranging from 350 to 700ºC, using the feldspar-water equation that O'Neil and Taylor (1967) proposed for a closed system (equation 2). For the $\delta^{18}O_{rock}^{final}$ value, the smectite-water equation (Savin and Lee, 1988) was used

$$\frac{w}{r} = \frac{\delta^{18}O_{rock}^{final} - \delta^{18}O_{rock}^{initial}}{\delta^{18}O_{H_2O}^{initial} - \delta^{18}O_{H_2O}^{final}} \quad (1)$$

(Ohmoto, 1986)

$$\Delta_{water}^{feldspar} = \frac{2.68 \times 10^6}{T^2} \quad (2)$$

(O'Neil and Taylor, 1967)

The water/rock ratios were calculated using those formulae and values. Positive results are considered meaningful (Table 8). Positive water/rock ratios are generally obtained for >650ºC plagioclase-water and <50ºC smectite-water equilibrium temperatures. As a result, if the formation temperature of the studied smectite is accepted to be ~40ºC, the water/rock ratio must be >1.0.

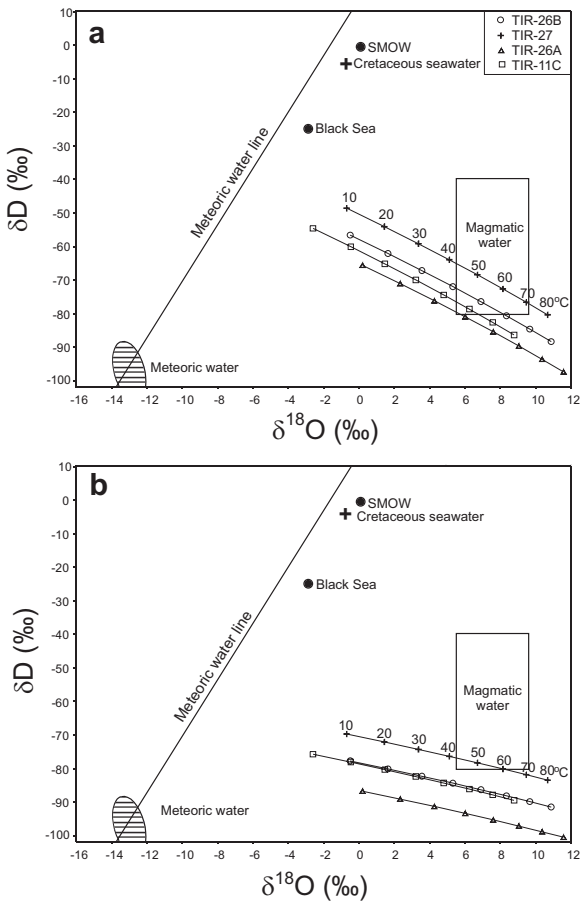

Figure 13. δD *vs.* $\delta^{18}O$ plot showing the calculated isotopic compositions of fluids in equilibrium with smectites from the Tirebolu area at different temperatures. (a) Calculation based on $10^3\ln\alpha(H)_{(montmorillonite\text{-}water)} = -45.3(10^3/T) + 94.7$ (Capuano, 1992). (b) Calculation based on $10^3\ln\alpha(H)_{(montmorillonite\text{-}water)} = -19.6(10^3/T) + 25$ (Yeh, 1980). In both a and b, the equation $10^3\ln\alpha(O)_{(smectite\text{-}water)} = +2.55(106/T^2) \pm 4.05$ (Sheppard and Gilg, 1996) was used. The shaded area and the cross represent the isotopic composition of the present-day meteoric water of the Black Sea region and Cretaceous seawater (Eslinger and Yeh, 1986), respectively.

DISCUSSION

Field observations (Zielinski, 1982; Senkayi *et al.*, 1984; Christidis *et al.*, 1995) and laboratory experiments (Mottl and Holland, 1978; Seyfried and Mottl, 1982; Shiraki *et al.*, 1987; Shiraki and Iijima, 1990) have shown that the alteration of volcanic glass, either to montmorillonite and beidellite-type smectites (based on XRD analyses of Mg-, K-, and Li-saturated clay fractions) or mordenite, involves mobilization of elements from and to the altered glass. Thus, the loss of alkalis and high Mg-activity promote the formation of smectite (Hay, 1977; Senkayi *et al.*, 1984). In open systems, the outside pore fluid acts as a sink, creating leaching conditions and providing a suitable environment for the formation of smectite (Senkayi *et al.*, 1984). Smectite develops on the dissolved surface (Dibble and Tiller, 1981), leading to pseudomorphic surfaces (Khoury and Eberl, 1979; Christidis *et al.*, 1995). Leaching of alkalis, accompanied by immobility of silica, may result in the development of a smectite + opal-CT paragenesis in the beidellite-bearing Tirebolu bentonite. When leaching is not effective, zeolites, such as mordenite in the Tirebolu bentonite, crystallize, usually from precursor gels (Mariner and Surdam,

https://doi.org/10.1346/CCMN.2010.0580112 Published online by Cambridge University Press

Table 8. Calculated water/rock ratio of the smectites from the Tirebolu (Giresun) bentonite samples at the time of formation. 5.5‰, 6.5‰, and 7.5‰ of $\delta^{18}O$ initial rock ratios were used in the calculations.

$\delta^{18}O_{rock}^{initial}$	Plagioclase-water equilibrium temperature (ºC)	Smectite-water equilibrium temperatures 10ºC	20ºC	30ºC	40ºC	50ºC	60ºC	70ºC	80ºC
5.5	350	−12.84	−10.33	−4.93	−3.46	−2.74	−2.31	−2.01	−1.81
	400	87.78	141.87	−6.60	−4.15	−3.14	−2.58	−2.22	−1.97
	450	47.55	−6.14	−9.44	−4.97	−3.57	−2.86	−2.42	−2.13
	500	15.14	−21.84	−16.97	−5.94	−4.02	−3.14	−2.62	−2.28
	550	10.51	2.32	59.50	−7.15	−4.50	−3.41	−2.80	−2.41
	600	8.47	13.14	−0.20	−8.73	−4.99	−3.68	−2.98	−2.54
	650	7.31	1355.41	−7.16	−11.01	−5.51	−3.94	−3.15	−2.66
	700	6.56	28.98	−13.16	−14.88	−6.06	−4.20	−3.30	−2.77
6.5	350	72.58	96.45	−6.32	−3.97	−3.00	−2.47	−2.12	−1.88
	400	24.78	−9.33	−10.32	−4.99	−3.53	−2.81	−2.37	−2.07
	450	11.09	−88.65	−55.03	−6.38	−4.13	−3.16	−2.61	−2.26
	500	7.97	9.23	−0.95	−8.45	−4.79	−3.53	−2.85	−2.43
	550	6.52	39.90	−10.05	−12.33	−5.55	−3.90	−3.09	−2.60
	600	5.68	17.10	−23.28	−26.18	−6.43	−4.28	−3.31	−2.76
	650	5.12	12.34	−353.39	27.26	−7.47	−4.67	−3.53	−2.90
	700	4.73	10.11	62.81	1.42	−8.76	−5.07	−3.75	−3.05
7.5	350	23.07	−9.11	−9.88	−4.76	−3.37	−2.68	−2.25	−1.97
	400	9.34	−41.49	32.03	−6.57	−4.11	−3.11	−2.55	−2.20
	450	6.59	235.96	−6.85	−10.09	−5.02	−3.59	−2.86	−2.42
	500	5.35	15.74	−23.93	−27.75	−6.18	−4.10	−3.17	−2.63
	550	4.64	10.36	−161.91	5.72	−7.77	−4.66	−3.48	−2.84
	600	4.19	8.19	3.83	−4.74	−10.26	−5.27	−3.79	−3.04
	650	3.87	7.00	73.69	−10.70	−15.30	−5.96	−4.11	−3.24
	700	3.63	6.24	22.50	−19.22	−37.78	−6.72	−4.42	−3.42

1970; Surdam, 1977; Taylor and Surdam, 1981; Steefel and Cappellen, 1990), while smectite generally forms in the initial stages of the alteration (Sheppard and Gude, 1973; Dibble and Tiller, 1981; Hay and Guldman, 1987). The leaching of Si from acidic rocks might lead to bentonites without silica polymorphs (Zielinski, 1982; Christidis and Scott, 1997). When excess Si remains in the system, opal-CT forms (Henderson *et al.*, 1971; Christidis and Dunham, 1997). Although the mineralogical and major chemical features of bentonite formations have been studied thoroughly, the mobility of trace elements, including lanthanides, with few exceptions (Zielinski, 1982; Elliott, 1993) have been examined thoroughly only in weathering profiles (Duddy, 1980; Banfield and Eggleton, 1989).

The pinkish coloration in the Tirebolu bentonite is probably due to the presence of Fe^{3+} oxides, which are incompatible with reducing conditions. Fe^{3+} oxide minerals may postdate the smectite and might have formed from oxidation of a precursor Fe-bearing phase, possibly pyrite or biotite. In addition, weathering may play an important role in colorization of bentonite due to the oxidation of structural Fe in smectite.

The origin and formation of clay occurrences in the Eastern Pontides (NE Turkey) were often thought to result from hydrothermal alteration due to the presence of massive sulfide deposits and young intrusive rocks (*e.g.* Kamitani, 1978). Recent studies reveal, however, that some clay occurrences in the region are related to *in situ* alteration *via* hydrolysis (Yalçın and Gümüşer, 2000; Abdioğlu and Arslan, 2005). In the Tirebolu bentonites, gradational contacts with surrounding pyroclastics, the presence of relict feldspar, biotite, devitrified glass shards, pumice fragments, and opal-CT, and the absence of

https://doi.org/10.1346/CCMN.2010.0580112 Published online by Cambridge University Press

epiclastic rock intercalation imply that the bentonites studied were developed *in situ* by alteration of pyroclastics of acidic to intermediate composition. The bentonites contain no fossils or organic material indicating a rapid and intense rate of pyroclastic eruption.

Furthermore, the absence of zonation, controlled by faults, and of Fe oxides and/or hydroxides and sulfur phases reveal diagenetic (*in situ*) alteration rather than hydrothermal alteration (Meunier, 1995, 2005; Inoue, 1995; Kadir and Akbulut, 2009; Kadir and Kart, 2009). The results are consistent with O- and H-isotopic values of the smectites and the formation-temperature assumptions.

The coexistence of smectite, mordenite, and kaolinite with feldspar; opal-CT in pyroclastics; and the micromorphological development of smectite between glassy volcanic materials, edging of mordenite fibers mostly by devitrified volcanic glass, and edging of kaolinite and kaolinite stacks by resorbed feldspar reveal the dissolution of glassy material and feldspar and re-precipitation as the mechanism. In shallow-marine environments, volcanic ashes are precursor materials of bentonites and, in this environment, bentonites have a diagenetic origin rather than a sedimentary one (Hillier, 1995; Kippli *et al.*, 2007). In other words, the interaction between pore water and rock is important. Alteration of glass includes textural and mineralogical changes. Therefore, alteration of volcanic glass begins with diffusion-controlled hydration and subsequent alkali ion exchange (Fisher and Schmincke, 1984). Chemically, Na is lost and K increases, but as alteration increases, K concentration decreases. Mass balance calculations and stable isotope studies show that the Tirebolu bentonite studied was formed in a shallow marine environment from a mixture of seawater and meteoric water at low temperatures *via* a slow diffusion rate and diagenesis.

According to Bohor and Triplehorn (1993), Al-silicate gels form smectites in basic environments in shallow marine waters with a small rate of leaching and excess Mg^{2+} ions. The chemical reaction related to their occurrence is given as follows:

$$\text{volcanic glass} \pm \text{feldspar} + H_2O \xrightarrow{\text{hydrolysis}} \text{hydrated Al-silica gel} \xrightarrow{\text{organic acids}} \text{smectite or zeolite} + \text{hydrated silica} + H_2O + \text{cations}$$

In associations with zeolite + smectite, zeolites and smectites are the first and last devitrification products of volcanic glass, respectively (Rice *et al.*, 1992). The absence of a large amount of carbonate rocks in association with the studied bentonites indicates that the Ca in the bentonite was not derived from the surrounding rocks and that the alkalinity of the environment was high at the time of clay fractionation. Gains in Mg indicate leaching in the solution and seawater circulation in the parent material. Despite the presence of exchangeable Mg in some of the samples containing smectite, which could indicate post clay-fraction alteration, the main source of Mg is believed to be the sea water in the shallow-marine environment that was present in the area during the Upper Cretaceous. The excess silica remaining from smectitization, zeolitization, and kaolinization may have been precipitated as opal-CT and quartz.

The presence of kaolinite in a few samples and the association of kaolinite crystals with platy and resorbed feldspar from the Tirebolu area indicate that feldspar degradation related to a tonstein bed was once associated with the bentonite, as formulated below (Bohor and Triplehorn, 1993):

$$\text{feldspar} \pm \text{volcanic glass} + H_2O \xrightarrow{\text{hydrolysis}} \text{hydrated Al-silica gel} \xrightarrow{\text{organic acids}} \text{kaolinite} + \text{hydrated silica} + H_2O + \text{cations}$$

The precise timing of alteration of the pyroclastics in the region cannot be determined from these data alone. Initial alteration of the pyroclastics appears to have occurred at or near the pyroclastics/water interface in contact with water ranging in salinity from brackish to marine, as occurred in the Wyoming example (*e.g.* Elzea, 1990). This alteration process may have continued for some time after the pyroclastic material was buried by other sediments.

CONCLUSIONS

Stratigraphic relations suggest that the bentonitic clays in the Tirebolu area were derived from Upper Cretaceous pyroclastics deposited in a shallow-marine environment. Bentonite formed by the *in situ* alteration of ash-sized pyroclastic materials of intermediate to acidic composition. Feldspar, quartz, biotite, pumice, and glass shards comprise the volcanogenic components. Clay, opal-CT, and mordenite are diagenetic phases. The clay minerals are characterized as Ca-smectite with a small amount of kaolinite and trace amounts of illite. Alteration of volcanic ash in an aqueous environment can lead to the formation of kaolinite (tonstein), smectite (bentonite), and/or mordenite. This is controlled by the volcanic eruption rate, the properties of the pyroclastic materials, such as chemical composition, grain size, and degree of alteration, as well as the salinity and/or alkalinity, pH, organic material content, and presence of inorganic suspended solids in the water in which the pyroclastic material falls. Removal of the mobile and immobile elements seems to be controlled by the degree of alteration during the conversion of pyroclastic materials to the bentonite.

ACKNOWLEDGMENTS

The study was supported financially by the Scientific Research Projects Fund of the Karadeniz Technical University in the framework of Project No. 2002.112.005.4. The authors are indebted to Professor

William Moll (Crystal Lake, Illinois, USA) and an anonymous reviewer for their extremely careful and constructive reviews, which significantly improved the quality of the paper. They are also grateful to Dr Richard Brown and Prof. Joseph W. Stucki for their insightful editorial comments and suggestions. Professor Eric Van Ranst is also thanked for his assistance during laboratory work by the second author at Ghent University, Belgium.

REFERENCES

Abdioğlu, E. (2002) Mineralogical, geochemical and genetic investigation of Kavaklar (Ünye-Fatsa, Ordu) area clay occurrences. MSc thesis, Karadeniz Technical University, Graduate School of Natural and Applied Sciences, Trabzon, Turkey, 132 pp.

Abdioğlu, E. and Arslan, M. (2005) Mineralogy, geochemistry and genesis of bentonites of the Ordu area, NE Turkey. *Clay Minerals*, **40**, 131–151.

Altaner, S.P. and Grim, R.E. (1990) Mineralogy, chemistry and diagenesis of tuffs in the Sucker Creek Formation (Miocene), Eastern Oregon. *Clays and Clay Minerals*, **38**, 561–572

Arslan, M., Kadir, S., Abdioğlu, E., and Kolaylı, H. (2006) Origin and formation of kaolin minerals in saprolite of Tertiary alkaline volcanic rocks, Eastern Pontides, NE Turkey. *Clay Minerals*, **41**, 599–619.

Arslan, M. and Aslan, Z. (2006) Mineralogy, petrography and whole-rock geochemistry of the Tertiary granitic intrusions in the Eastern Pontides, Turkey. *Journal of Asian Earth Sciences*, **27**, 177–193.

Arslan, M., Tüysüz, N., Korkmaz, S., and Kurt, H. (1997) Geochemistry and petrogenesis of the Eastern Pontide Volcanic Rocks, Northeast Turkey. *Chemie der Erde/ Geochemistry*, **57**, 157–187.

Arslan, M., Boztuğ, D., Şen, C., Kolaylı, H., Temizel, İ., and Abdioğlu, E. (2007) *Petrogenesis and geodynamic evolution of the southern zone Eocene volcanics, Eastern Pontides, NE Turkey (Turkish with English Abstract)*. TÜBİTAK-ÇAYDAG 103Y012 Project Report, 119 pp.

Balderer, W. (1999) *Application of Isotope Techniques in Hydrogeology*. Short Course Notes, İstanbul, Turkey, 79 pp.

Banfield, J.F. and Eggleton, R.A. (1989) Apatite replacement and rare earth mobility, fractionation, and fixation during weathering. *Clay Minerals*, **37**, 113–127.

Bohor, B.F. and Triplehorn, D.M. (1993) Tonsteins: altered volcanic ash layers in coal-bearing sequences. *Geological Society of America Special Paper*, **285**, 44 pp.

Buhmann, C., Fey, M.V. and Villiers, J.M. (1985) Aspects of X-ray identification of swelling clay minerals in soils and sediments. *South African Journal of Scienc*e, **81**, 505–509.

Brindley, G.W. (1980) Quantitative X-ray analysis of clays. Pp. 411–438 in: *Crystal Structures of Clay Minerals and their X-ray Identification* (G.W. Brindley and G. Brown, editors). Monograph **5**, Mineralogical Society, London.

Caballero, E., Jimenez de Cisneros, C., Huertas, F.J., Huertas, F., Pozzuoli, A., and Linares, J. (2005) Bentonites from Cabo de Gata, Almeria Spain; a mineralogical and geochemical overview. *Clay Minerals*, **40**, 463–480.

Capuano, R.M. (1992) The temperature dependence of hydrogen isotope fractionation between clay minerals and water: evidence from a geopressured system. *Geochimica et Cosmochimica Acta*, **56**, 2547–2554.

Christidis, G.E. (1998) Comparative study of the mobility of major and trace elements during alteration of an andesite and a rhyolite to bentonite, in the islands of Milos and Kimolos, Aegean, Greece. *Clays and Clay Minerals*, **46,** 379–399.

Christidis, G. and Dunham, A.C. (1997) Compositional variations in smectites. Part II: Alteration of acidic precursors, a case study from Milos Island, Greece. *Clay Minerals*, **32**, 253–270.

Christidis, G.E. and Huff, W.D. (2009) Geological aspects and genesis of bentonites. *Elements*, **5**, 93–98.

Christidis, G. and Scott, P.W. (1997) The origin and control of colour of white bentonites from the Aegean islands of Milos and Kimolos, Greece. *Mineralium Deposita*, **32**, 271–279.

Christidis, G., Scott, P.W., and Marcopoulast, T. (1995) Origin of the bentonite deposits of Eastern Milos and Kimalos, Greece: geological, mineralogical and geochemical evidence. *Clays and Clay Minerals*, **43**, 63–77.

Churchman, G.J. (1990) Relevance of different intercalation tests for distinguishing halloysite from kaolinite in soils. *Clays and Clay Minerals*, **38**, 591–599.

Churchman, G.J. and Gilkes, R.J. (1989) Recognition of intermediates in the possible transformation of halloysite to kaolinite in weathering profiles. *Clay Minerals*, **24**, 579–590.

Clayton, R.N. and Mayeda, T. (1963) The use of bromine pentafluoride in the extraction of oxygen from oxides and silicates for isotopic analysis. *Geochimica et Cosmochimica Acta*, **27**, 47–52.

Çoban, F. and Ece, Ö.I. (1999) Fe^{3+}-rich montmorillonite–beidellite series in Ayvacık bentonite deposit, Biga Peninsula, Northwest Turkey. *Clays and Clay Minerals*, **47**, 165–173.

Craig, H. and Gordon, L.I. (1965) Deuterium and oxygen-18 variations in the ocean and the marine atmosphere. Pp. 9–130 in: *Stable Isotopes in Oceanographic Studies and Paleotemperatures* (E. Tongiorgi, editor). Consiglia Nazionale dele Ricerche, Laboratorio di Geologica Nucleare, Italy.

Ddani, M., Meunier, A., Zahraoui, M., Beaufort, D., El Wartiti, M., Fontaine, C., Boukili, B., and El Mahi, B. (2005) Clay mineralogy and chemical composition of bentonites from the Gourougou volcanic massif, Northeast Morocco. *Clays and Clay Minerals*, **53**, 250–267.

Dibble, J.R. and Tiller, W.A. (1981) Kinetic model of zeolite paragenesis in tuffaceous sediments. *Clays and Clay Minerals*, **29**, 323–330.

Dixon, C.J. and Pereira, J. (1974) Plate tectonics and mineralization in the Tethyan Region. *Mineralium Deposita*, **9**, 185–198.

Duddy, L.R. (1980) Redistribution and fractionation of rare-earth and other elements in a weathering profile. *Chemical Geology*, 30, 363–381.

Elliot, W.C. (1993) Origin of the Mg smectite at the Cretaceous/Tertiary (K/T) boundary at Stevns Klint, Denmark. *Clays and Clay Minerals*, **41**, 442–452.

Elzea, J.M. (1990) Geology, geochemistry, selected physical properties and genesis of the Cretaceous Clay Spur bentonite in Wyoming and Montona, USA. PhD thesis, Indiana University, USA. 201 pp.

Eslinger, E.V. and Yeh, H.W. (1986) Oxygen and hydrogen isotope geochemistry of Cretaceous bentonites and shales from disturbed belt, Montana. *Geochimica et Cosmochimica Acta*, **50**, 59–68.

Faure, G. and Mensing, T.M. (2004) *Isotopes: Principles and Applications (3rd edition)*. John Wiley, New York, 897 pp.

Fisher, R.V. and Schmicke, H.U. (1984) *Pyroclastic Rocks*. Springer-Verlag, New York, 472 pp.

Gedik, İ. (2001) Microplates (terranes) of Turkey and their types and the importance of strike-slip-faults in building geological structures. Pp. 186 in: *Fourth International Turkish Geology Symposium Abstracts*, Adana, Turkey.

Gedik, İ. (2003) Türkiye jeolojisinin oluşumunda 'terrane' yapısının önemi. Pp. 281–283 in: *56th Geological Congress of Turkey Abstracts*, Ankara, Turkey.

Grim, R.E. and Güven, N. (1978) *Bentonites, Geology, Mineralogy, Properties and Uses.* Elsevier, Amsterdam, pp. 13–137.

Gültekin, F. (1999) Gümüşhane ve Bayburt Yöresi Mineralli Su Kaynaklarının Hidrokimyası ve İzotopik Özellikleri. PhD thesis, Karadeniz Technical University, Turkey, 188 pp.

Güven, N. (2009) Bentonites; clays for molecular engineering. *Elements*, **5**, 89–92.

Harvey, C.C. and Lagaly, G. (2006) Conventional applications. Pp. 499–540 in: *Handbook of Clay Science* (F. Bergaya, B.K.G. Theng, and G. Lagaly, editors). Developments in Clay Science, **1**, Elsevier, Amsterdam.

Hay, R.L. (1977) Geology of zeolites in sedimentary rocks. Pp. 53–64 in: *Mineralogy and Geology of Natural Zeolites* (F.A. Mumpton, editor). Reviews in Mineralogy, **4**. Mineralogical Society of America, Washington, D.C.

Hay, R.L. and Guldman, S.G. (1987) Diagenetic alteration of silisic ash in Searles lake, California. *Clays and Clay Minerals*, **35**, 449–457.

Henderson, J.H., Jackson, M.L., Syers, J.K, Clayton, R.N., and Rex, R.W. (1971) Cristobalite authigenic origin in relation to montmorillonite and quartz origin in bentonite. *Clays and Clay Minerals*, **19**, 229–238.

Hillier, S. (1995) Erosion, sedimentation and sedimentary origin of clays. Pp. 162–219 in: *Origin and Mineralogy of Clays* (B. Velde, editor). Springer-Verlag, New York.

Inoue, A. (1995) Formation of clay minerals in hydrothermal environments. Pp. 268–329 in: *Origin and Mineralogy of Clays, Clays and the Environment* (B. Velde, editor). Springer-Verlag, Berlin.

Jeans, C.V., Wray, D.S., Merriman, R.J., and Fisher, M.J. (2000) Volcanogenic clays in Jurassic and Cretaceous strata of England and the North Sea Basin. *Clay Minerals*, **35**, 25–55.

Kadir, S. and Akbulut, A. (2009) Mineralogy, geochemistry and genesis of the Taşoluk kaolinite deposits in pre-Early Cambrian metamorphites and Neogene volcanites of Afyonkarahisar, Turkey. *Clay Minerals*, **44**, 89–112.

Kadir, S. and Kart, F. (2009) The occurrence and origin of the Söğüt kaolinite deposits in the Paleozoic Saricakaya granite-granodiorite complexes and overlying Neogene sediments (Bilecik, Northwestern Turkey). *Clays and Clay Minerals*, **57**, 311–329.

Kamitani, M. (1978) *Kaolinite, sericite and montmorillonite deposits in the Eastern Blacksea region*. General Directorate of Mineral Research & Exploration, Ankara, Turkey, 24 pp.

Khoury, H.N. and Eberl, D.D. (1979) Bubble-wall shards altered to montmorillonite. *Clays and Clay Minerals*, **27**, 291–292.

Kippli, T., Kippli, E., Kalleste, T., Hints, R., Somelar, P., and Kirsimae, K. (2007) Altered volcanic ash as an indicator of marine environment, reflecting pH and sedimentation rate; example from the Ordovician Kinnekulle Bed of Baltoscandia. *Clays and Clay Minerals*, **55**, 177–188.

MacKenzie, R.C. (1957) Thermal methods. Pp. 1–22 in: *Differential Thermal Investigation of Clays* (R.C. Mackenzie, editor). Monograph **2**, Mineralogical Society, London.

MacLean, W.H. and Kranidiotis, P. (1987) Immobile elements as monitors of mass transfer in hydrothermal alteration: Phelps Dodge massive sulfide deposits, Matagami, Quebec. *Economic Geology*, **2**, 951–962.

Mariner, R.H. and Surdam, R.C. (1970) Alkalinity and formation of zeolites in saline, alkaline lakes. *Science*, **170**, 977–980.

Meunier, A. (1995) Hydrothermal alteration by veins. Pp. 247–267 in: *Origin and Mineralogy of Clays, Clays and the Environment* (B. Velde, editor). Springer-Verlag, Berlin.

Meunier, A. (2005) *Clays*. Springer, Heidelberg, 472 pp.

Moore, D.M. and Reynolds, R.C. (1989) *X-ray Diffraction and the Identification and Analysis of Clay Minerals*. Oxford University Press, New York, 332 pp.

Mottl, M.J. and Holland, H.D. (1978) Chemical exchange during hydrothermal alteration of basalt by seawater, I. Experimental results for major and minor components of seawater. *Geochimica et Cosmochimica Acta*, **42**, 1103–1115.

Murray, H.H. (1991) Overview-clay mineral application. *Applied Clay Science*, **5**, 379–395.

Murray, H.H. (1999) Applied clay mineralogy today and tomorrow. *Clay Minerals*, **34**, 39–49.

Murray, H.H. (2007) *Applied Clay Mineralogy, Occurrences, Processing and Application of Kaolins, Bentonites, Palygorskite-Sepiolite, and Common Clays*. Developments in Clay Science, **2**. Elsevier, USA, 180 pp.

Ohmoto, H. (1986) Stable isotope geochemistry of ore deposits. Pp. 491–559 in: *Stable Isotopes in High Temperature Geological Processes* (J.W. Valley, H.P. Taylor Jr., and J.R. O'Neil, editors). Reviews in Mineralogy **16**, Mineralogical Society of America, Washington, DC.

Okay, A.I. and Şahintürk, Ö. (1997) Geology of the Eastern Pontides. Pp. 291–311 in: *Regional and Petroleum Geology of the Black Sea and Surrounding Region* (A.G. Robinson, editor). AAPG Memoir, **68**, American Association of Petroleum Geology, Tulsa, Oklahoma.

O'Neil, J.R. and Taylor, H.P. (1967) The oxygen isotope and cation exchange chemistry of feldspars. *American Mineralogist*, **52**, 1414–1437.

Paterson, E. and Swaffield, R. (1987) Thermal analysis. Pp. 99–132 in: *A Handbook of Determinative Methods in Clay Mineralogy* (M.J. Wilson, editor). Blackie and Sons Limited, Glasgow, UK.

Rice, S.B., Papke, K.G., and Vaughan, D.E. (1992) Chemical controls on ferrierite crystallization during diagenesis of silicic pyroclastic rock near Lovelock, Nevada. *American Mineralogist*, **77**, 314–328.

Righi, D. and Meunier, A. (1995) Origin of clays by rock weathering and soil formation. Pp. 43–157 in: *Origin and Mineralogy of Clays* (B. Velde, editor). Springer Verlag, Berlin.

Savin, S.M. and Epstein, S. (1970) The oxygen and hydrogen isotope geochemistry of clay minerals. *Geochimica et Cosmochimica Acta*, **34**, 25–42.

Savin, S.M. and Lee, M. (1988) Isotopic studies of phyllosilicates. Pp. 189–223 in: *Hydrous Phyllosilicates* (S.W. Bailey, editor). Reviews in Mineralogy, **19**, Mineralogical Society of America, Washington DC.

Savin, S.M., Douglas, R.G., and Stehli, F.G. (1975) Tertiary marine paleotemperatures. *Geological Society of America Bulletin*, **86**, 1499–1510.

Şen, C. (2007) Jurassic volcanism in the Eastern Pontides: Is it rift related or subduction related? *Turkish Journal of Earth Sciences*, **16**, 523–539.

Şen, C., Arslan, M., and Van, A. (1998) Geochemical and petrological characteristics of the Eastern Pontide Eocene (?) alkaline volcanic province, NE Turkey. *Turkish Journal of Earth Sciences*, **7**, 231–239.

Şengör, A.M.C. and Yılmaz, Y. (1981) Tethyan evolution of Turkey: a plate tectonic approach. *Tectonophysics*, **75**, 181–241.

Senkayi, A.L., Dixon, J.B., Hossner, L.R., Abder-Ruhman, M., and Fanning, D.S. (1984) Mineralogy and genetic relationships of tonstein, bentonite, and lignitic strata in the Eocene Yegua formation of East-Central Texas. *Clays and Clay Minerals*, **32**, 259–271.

Seyfried, W.E., Jr. and Mottl, M.J. (1982) Hydrothermal alteration of basalt under seawater-dominated conditions. *Geochimica et Cosmochimica Acta*, **46**, 985–1002.

Shackleton, N.J. and Kennett, J.P. (1975) Paleotemperature history of the Cenozoic and the initiation of Antarctic

glaciation: oxygen and carbon isotope analyses in DSDP sites 277, 279, and 281. Pp. 743–755 in: *Initial Reports of the Deep Sea Drilling Project* (J.P. Kennett, R.E. Houtz *et al*., editors). U.S. Government Printing Office, Washington.

Sheppard, S.M.F. and Gilg, H.A. (1996) Stable isotope geochemistry of clay minerals. *Clay Minerals*, **31**, 1–24.

Sheppard, R.A. and Gude, A.J. (1973) *Zeolites and Associated Authigenic Silicate Minerals in Tuffaceous Rocks of the Big Sandy Formation, Mohave County, Arizona*. U.S. Geological Survey, Professional Paper **830**, 36 pp.

Sheppard, S.M.F., Nielsen, R.L., and Taylor, H.P., Jr. (1969) Oxygen and hydrogen isotope ratios of clay minerals from porphyry copper deposits. *Economic Geology*, **64**, 755–777.

Shiraki, R. and Iijima, T. (1990) Na-K ion exchange reaction between rhyolitic glass and (Na,K)Cl aqueous solution under hydrothermal conditions. *Geochemica et Cosmochimica Acta*, **54**, 2923–2931.

Shiraki, R., Sakai, H., Endo, M., and Kishima, N. (1987) Experimental studies on rhyolite- and andesite-seawater interactions at 300ºC and 1000 bars. *Geochemical Journal*, **21**, 139–148

Steefel, C.I. and Van Cappellen, P. (1990) A new kinetic approach to modeling water-rock interaction: The role of nucleation, precursors and Ostwald ripening. *Geochemica et Cosmochimica Acta*, **54**, 2657–2677.

Sun, S.S. and McDonough, W.F. (1989) Chemical and isotopic systematics of oceanic basalts: implications for mantle composition and processes. Pp. 313–345 in: *Magmatism in Ocean Basins* (A.D Saunders. and M.J. Norry, editors). Special Publication, **42**, Geological Society, London.

Surdam, R.C. (1977) Zeolites in closed hydrologic systems. Pp. 65–91 in: *Mineralogy and Geology of Natural Zeolites* (F.A. Mumpton, editor). Mineralogical Society of America, Washington, D.C.

Taylor, H.P. Jr. (1979) Oxygen and hydrogen isotope relationships in hydrothermal mineral deposits. Pp. 236–277 in: *Geochemistry of Hydrothermal Ore Deposits* (H.L. Barnes, editor). John Wiley, New York.

Taylor, S.R. and McLennan, S.M. (1985) *The Continental Crust: Its Composition and Evolution*. Blackwell, Oxford, UK, 312 pp.

Taylor, M.W. and Surdam, R.C. (1981) Zeolite reactions in the tuffaceous sediments at Teels Marsh, Nevada. *Clays and Clay Minerals*, 29, 341–352.

Temizel, İ. and Arslan, M. (2008) Petrology and geochemistry of Tertiary volcanic rocks from the İkizce (Ordu) area, NE Turkey: Implications for the evolution of the eastern Pontide paleo-magmatic arc. *Journal of Asian Earth Sciences*, **31**, 439–463.

Uno, Y. and Takeshi, H. (1979) Exchange cations and structural formulae of montmorillonites in the Nakajo acid clay deposits, Nigata prefecture. *Journal of the Mineralogical Society of Japan*, **14**, 90–103.

Uz, B. and Bacak, G. (2001) Mineralogical, physico-chemical and geological characteristics of the Kargalı bentonite deposits (Kocaeli-Turkey). Pp. 307–319 in: *4th International Symposium on Eastern Mediterranean Geology* Proceedings, Isparta, Turkey.

Uz, B., Esenli, F., Özdamar, Ş., Esenli, V., and Suner, F. (2003) The comparison of ordering opal structure in two different bentonite occurrences. *Journal of the Geological Society of India*, **62**, 478–484.

Van Ranst, E. (1998) *Analysis and Dynamics of Clays*. Lecture Notes, Laboratory of Soil Science, Ghent University, 241 pp.

Wilson, M.J. (1987) X-ray powder diffraction methods. Pp. 26–98 in: *A Handbook of Determinative Methods in Clay Mineralogy* (M.J. Wilson, editor). Blackie, Glasgow, UK.

Winchester, J.A. and Floyd, P.A. (1977) Geochemical discrimination of different magma series and their differentiation products using immobile elements. *Chemical Geology*, **20**, 245–252.

Yalçın, H. and Gümüşer, G. (2000) Mineralogical and geochemical characteristics of Late Cretaceous bentonite deposits of the Kelkit Valley Region, Northern Turkey. *Clay Minerals*, **35**, 807–825.

Yeh, H.W. (1980) D/H ratios and late stage dehydration of shales during burial. *Geochemica et Cosmochimica Acta*, **44**, 341–352.

Yui, T. and Chang, S. (1999) Formation conditions of vesicle/fissure filling smectites in Penghu basalts: a stable-isotope assessment. *Clay Minerals*, **34**, 381–393.

Zielinski, R.A. (1982) The mobility of uranium and other elements during alteration of rhyolite ash to montmorillonite: A case study in the troublesome formation, Colorado, USA. *Chemical Geology*, **35**, 185–204.

(*Received 24 July 2008; revised 23 October 2009; Ms. 185; A.E. R.W. Brown*)